Angewandte Reviews

DOI: 10.1002/anie.201108690

Supramolecular Chemistry

Molecular Assemblies of Perylene Bisimide Dyes in Water

*Daniel Görl, Xin Zhang, and Frank Würthner**

Keywords:
dyes/pigments · hydrophobic interactions · perylene bisimides · π stacking · supramolecular chemistry

Dedicated to Professor François Diederich on the occasion of his 60th birthday

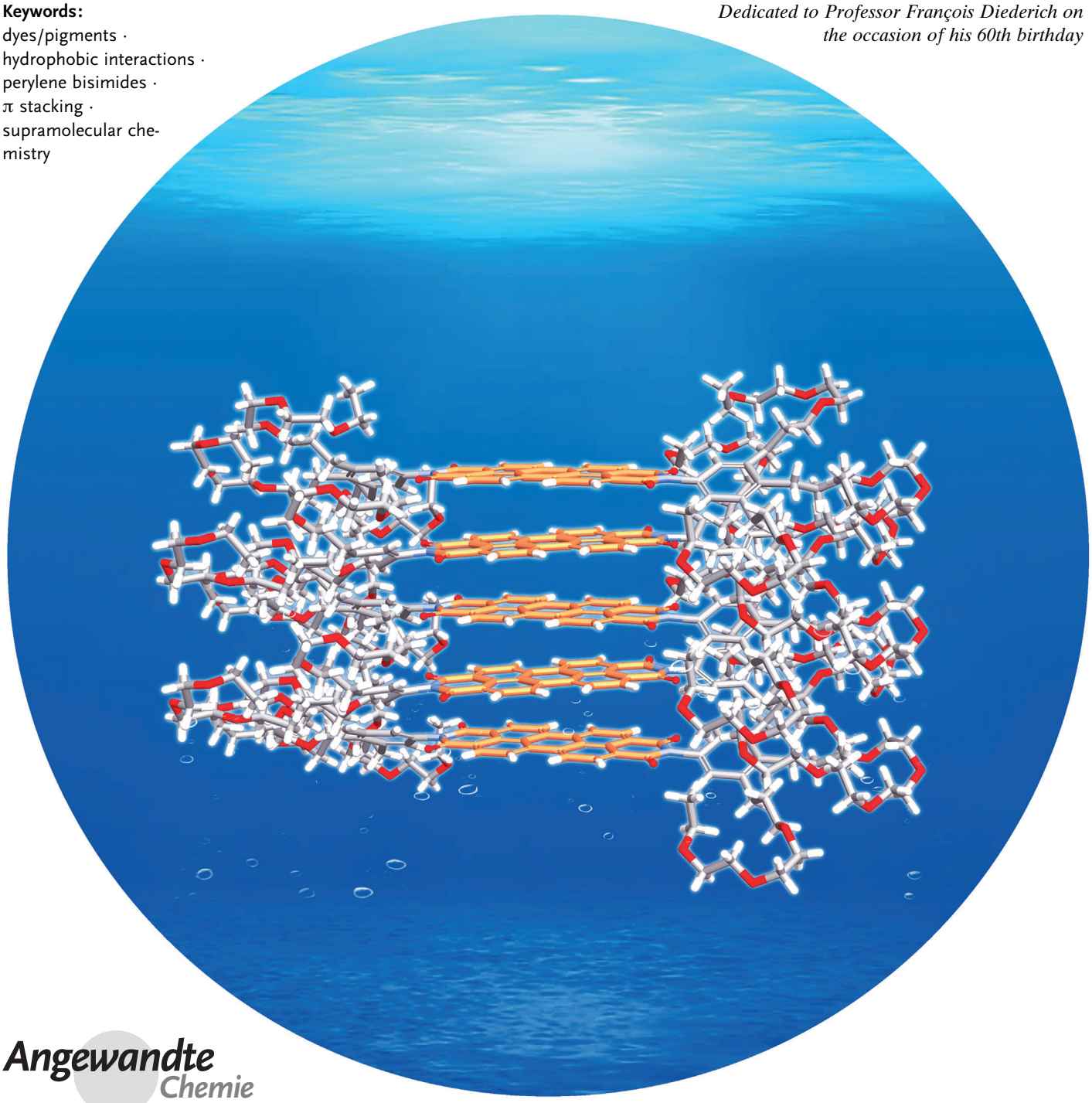

Angewandte Chemie

Angewandte International Edition Chemie

Perylene bisimides are among the most valuable functional dyes and have numerous potential applications. As a result of their chemical robustness, photostability, and outstanding optical and electronic properties, these dyes have been applied as pigments, fluorescence sensors, and n-semiconductors in organic electronics and photovoltaics. Moreover, the extended quadrupolar π system of this class of dyes has facilitated the construction of numerous supramolecular architectures with fascinating photophysical properties. However, the supramolecular approach to the formation of perylene bisimide aggregates has been restricted mostly to organic media. Pleasingly, considerable progress has been made in the last few years in developing water-soluble perylene bisimides and their application in aqueous media. This Review provides an up-to-date overview on the self-assembly of perylene bisimides through π–π interactions in aqueous media. Synthetic strategies for the preparation of water-soluble perylene bisimides and the influence of water on the π–π stacking of perylene bisimides as well as the resulting applications are discussed.

From the Contents

1. Introduction

Water is essential! The specific properties of water make it indispensable for life. As a solvent of nature, it not only serves as an environment for the vital processes of life but is also involved in numerous biochemical reactions. In accordance with its biological significance, water is also called the "molecule of life", "matrix of life", and other similar terms.[1] Water is distinguished from other solvents by its anomalous behavior in terms of many physical properties that originate from its molecular construction. As a consequence of its geometrical structure, water forms infinite, branched networks through hydrogen bonds.[2] This has two major consequences for supramolecular chemistry, in terms of noncovalent interactions, in this structured solvent. On the one hand, hydrogen bonds are, in particular, created in a hydrophobic microenvironment and they play an important role in the folding of biomacromolecules (e.g. proteins and DNA) and also in biological self-assembly. On the other hand, the hydrophobic effect results in an exceptionally strong attraction between hydrophobic molecules or surfaces in water, and constitutes the basis not only for processes such as the nonmiscibility of oil and water, but also the formation of biological structures such as membranes as well as protein folding.[3] Even today, the seemingly trivial concept of the hydrophobic effect is not completely understood. This is due to the complex interplay between enthalpy ($\Delta H°$) and entropy ($\Delta S°$) contributions to the change in the standard Gibbs free energy ($\Delta G° = \Delta H° - T\Delta S°$) on hydration of hydrophobic molecules in water, since the energetic contributions depend not only on the temperature and pressure, but also on the size of the hydrophobic surface and the concentration of the solute.[4] The thermodynamic explanation of this phenomenon also lies in the extended hydrogen-bonding network of water, since such a network is interrupted by the dissolved substrate, and thus a differentiation should be made between small and large substances.[5]

No hydrogen bonds need to be broken when small molecules (< 1 nm) are dissolved in water. In this case, the water molecules only reorient so that the hydrogen bonds enclose the solute. This solvation process, therefore, does not require a significant enthalpic contribution, and thus the free energy of solvation is dominated by entropy. However, this effect vanishes along with the loss of hydrogen bonds on increasing the temperature until the boiling point is approached. However, in the case of extended hydrophobic surfaces, such as with aggregates and nanoparticles, under no circumstances can the hydrogen-bonding network be sustained. The decrease in the number of hydrogen bonds along the extended hydrophobic surfaces (less hydrogen bonds for the water molecules that are localized at the interface than those in the bulk water) now leads to a situation in which the change in the free energy for the solvation of these objects is determined by enthalpic contributions. As a consequence of the dependence of these enthalpic and entropic solvation factors on temperature, size, and structural features, an intricate situation with counter effects arises for the clustering of hydrophobic objects in water.[6] The driving force for the aggregation of the majority of amphiphilic molecules in water most likely arises from a combination of dominant entropic contributions from the solvation of the molecular building blocks and a dominant enthalpic contribution for the solvation of the extended aggregates to the standard Gibbs free energy. Under these conditions, the self-assembly is often

[*] D. Görl, Dr. X. Zhang, Prof. Dr. F. Würthner
Universität Würzburg, Institut für Organische Chemie and Center for Nanosystems Chemistry
Am Hubland, 97074 Würzburg (Germany)
E-mail: wuerthner@chemie.uni-wuerzburg.de

enhanced on increasing the temperature, and thus can not accurately be described as entropy-driven.[5]

The hydrophobic effect plays a decisive role in many important phenomena, such as molecular self-assembly, formation of micelles and biological membranes, and protein folding.[7–9] Although several noncovalent interactions, for example, hydrogen bonding, are specific and directional in the formation of supramolecular structures, this is usually not the case for hydrophobic interactions. Therefore, the structures of supramolecular aggregates formed in water can not be predicted as easily as in the case of organic media. Nevertheless, water offers many opportunities and advantages as a solvent for supramolecular chemistry compared with organic media. On the one hand, the hydrophobic effect results in increased interactions between hydrophobic π surfaces, for example, aromatic compounds, and thus the desired recognition and self-assembly processes leading to extended architectures may already occur in dilute solutions. On the other hand, enormous opportunities may arise from the interaction of such supramolecular structures with biological materials in water.

In this regard, aggregates of π-conjugated dye molecules are, in particular, the focus of interest. Inspired by natural supramolecular structures such as, for example, the DNA double helix or (bacterio)chlorophyll arrays of the photosynthesis apparatus, numerous functional architectures based mainly on π-conjugated dye molecules have been synthesized through noncovalent interactions, particularly π–π interactions. Supramolecular architectures with highly promising optical and electronic properties, which are not inherent to the respective individual molecules, could be generated by this approach, and thus facilitated, for example, efficient energy and electron transfer.[10] Such self-assembled materials find applications in organic electronics[11] and artificial photosynthesis.[12] The π–π interactions between individual building blocks used for self-assembly reflect the sum of noncovalent interactions including electrostatic and dispersion interactions as well as attractive (charge transfer (CT)) and repulsive orbital interactions.[13] Since the individual contributions are strongly solvent-dependent, especially in water, this may lead to large binding constants because the hydrophobic effect makes the largest contribution to the standard Gibbs free energy for aggregate formation.

It turned out to be a great challenge to generate such molecular aggregates in aqueous media, as this requires the introduction of an adequate number of polar, water-solubility-mediating functionalities into the parent building blocks. This has been achieved for one-dimensional π-conjugated oligomers such as *p*-phenylenes,[14] *p*-oligophenylenevinylenes,[15] and oligophenyleneethinylenes[16] as well as for two-dimensional, extended polycyclic aromatic compounds such as triphenylenes[17] and hexabenzocoronenes.[18]

Remarkably, the prospect of using perylene bisimide (PBI) dyes[19,20] (Figure 1) to construct supramolecular aggregates in aqueous medium has been approached relatively late. The targeted construction of π–π-stacked structures of PBIs was initially restricted to organic solvents.[19]

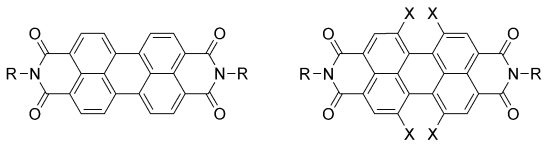

Figure 1. General chemical structures of perylene bisimides (PBIs) without (left) and with (right) substituents in the bay positions.

Water-soluble PBIs with ionic substituents at the imide positions that exhibited intensive fluorescence in water, for example, PBIs **1** and **2** (Figure 2), were already known in the 1980s and 1990s.[21] Moreover, Ford showed that PBI **1a** ($n = 1$) containing two glycine residues forms aggregates in basic aqueous solutions whose fluorescence is quenched nearly completely compared to that of the respective monomers (fluorescence quantum yield $\Phi_f \approx 100\,\%$).[21b] Müllen and coworkers considerably expanded the potential of water-soluble PBIs by introducing ionic groups at the bay positions, which effectively prevent aggregation even in water through electrostatic shielding and steric hindrance. As a result, appreciable fluorescence quantum yields for PBIs such as **3** could be achieved in water.[22] A more effective shielding by dendrons resulted in strongly emitting PBIs such as **4**.[23] These and other similar PBI molecules and their application for protein labeling or single-molecule spectroscopy are not the focus of this Review, and at this point we refer the interested reader to a recently published excellent review article on this topic by Weil et al.[24]

This Review, in contrast, deals with π-stacked supramolecular structures of perylene bisimides in water. This is still a relatively young research field, which may seem

Daniel Görl was born in 1984 in Erlenbach/Main, Germany. He studied Chemistry at the University of Würzburg. In 2009 he joined the group of Prof. Würthner, where he is currently pursuing his PhD on amphiphilic perylene bisimides.

Xin Zhang was born in 1972 in the Jilin province, China. He studied Chemistry at Jilin University, China (bachelor degree 1995). Subsequently he completed his PhD in the group of Prof. Fumian Li at Peking University in 2003, followed by two years of research work in the group of Prof. Zi-Chen Li. He was awarded an Alexander von Humboldt postdoctoral fellowship from March 2006 to August 2007 to continue his scientific career in the research group of Prof. Würthner at the University of Würzburg. Since 2007, he has been working as a research associate in Würzburg.

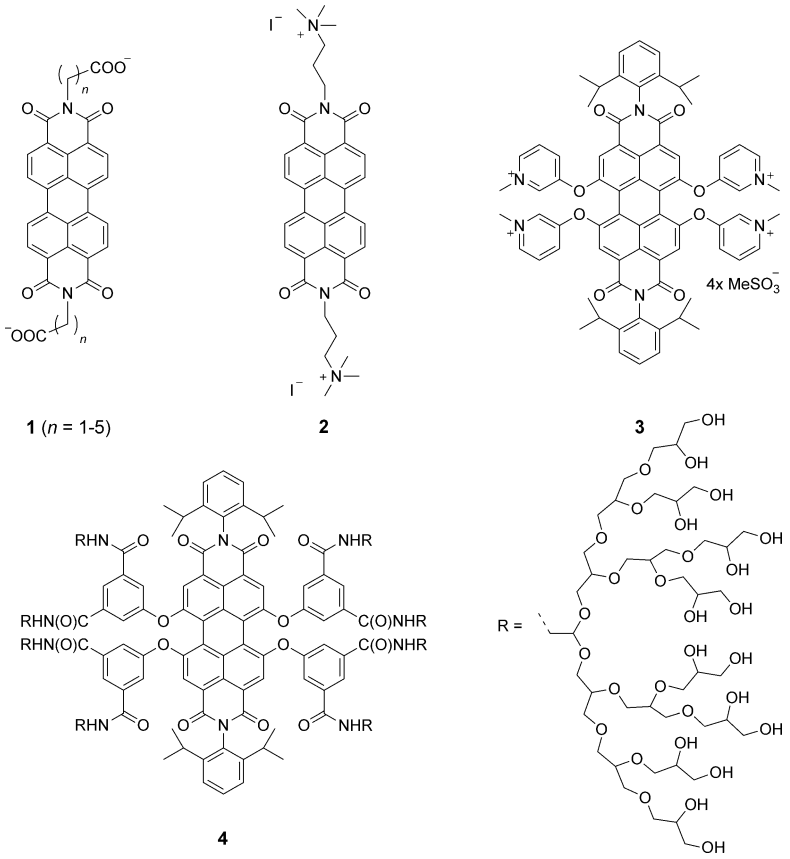

Figure 2. Chemical structures of water-soluble PBIs **1**–**4**.

surprising, but perylene bisimides seem to be suitable for many applications in aqueous media. One might expect on considering the parent structure of perylene bisimides that the carbonyl acceptors of the imide groups would promote water solubility through hydrogen bonding, which would come into play particularly in π–π aggregates because of the peripheral position of the carbonyl groups being in contact with the aqueous medium. Moreover, the high quadrupole moment of the perylene scaffold should have a positive influence on the water solubility.

In fact, by using very similar concepts known for organic media, perylene bisimides can be derivatized for the directed assembly of supramolecular aggregates in water.[15,25–27] Thus, by simple incorporation of hydrophilic side groups in the imide substituents, PBI derivatives could be generated that already aggregate in highly dilute solutions with binding constants greater than $10^8\,M^{-1}$ and still possess outstanding solubility at high concentrations.[26,27] In the following, fundamental studies and the resulting applications will be discussed.

Frank Würthner, born in 1964, studied Chemistry at the University of Stuttgart (Germany) where he obtained his PhD with F. Effenberger. After postdoctoral research at MIT in Cambridge (USA, with J. Rebek, Jr.), and two years at BASF SE in Central Research (Ludwigshafen, Germany), he completed his Habilitation in Organic Chemistry at the University of Ulm (2001). In 2002 he became Professor of Organic Chemistry at the University of Würzburg, where he is also an executive director of the Wilhelm-Conrad Röntgen Research Center for Complex Material Systems (since 2006) and founder of the Center for Nanosystems Chemistry (2010).

2. Basic Aspects of π–π Stacking of PBIs in Water

The fundamental question is how does water affect the interaction of PBI molecules, or how pronounced is its influence on the structure and stability of PBI aggregates? To answer this question, a deeper understanding of solvent effects on the π-π aggregation of PBIs is essential. The effect of the solvent on the binding constants of the π–π aggregation of perylene bisimides has been investigated in great detail by our research group for core-unsubstituted PBIs that undergo isodesmic (i.e. described by a single binding constant K, also known as the equal K model)[26] self-assembly into columnar stacks. We have correlated the obtained standard Gibbs free energies $-\Delta G°$ for π–π stacking with solvent permittivity as well as with the empirical polarity scales of solvents.[27] Quantum chemical calculations have shown that the π–π interaction of PBI dyes is influenced by different forces, of which the electrostatic and dispersion interactions contribute the most.[28] Scanning force and transmission electron microscopy (TEM) studies revealed a one-dimensional columnar arrangement of the aggregates of PBIs **5** and **6** (Figure 3) in organic[29] (**5**) as well as in aqueous[30] (**6**) environment.

On the basis of the experimental data for PBIs **5** and **6**, which as a result of their hydrophobic and hydrophilic imide substituents, respectively, cover complimentary solvent polarity ranges, evidence for a biphasic aggregation behavior of these dyes was obtained (Figure 4a).[27] Thus, the aggregation constants and the related standard free energies $-\Delta G°$ for **5**, whose hydrophobic imide substituents impart a high solubility in nonpolar solvents, decrease with increasing solvent polarity, whereas the aggregation constants and $-\Delta G°$ values for **6** in polar solvents, which are now suitable solvents for this PBI because of its hydrophilic imide substituents, increase again as the solvent polarity increases.[27] A special effect arising from alkyl or oligoethylene glycol chains does not appear to exist, since identical values were obtained for **5** and **6** in several solvents. The results for **5** reveal that, besides dispersion forces, electrostatic interactions also provide a significant contribution to the binding strength between PBI molecules in nonpolar solvents, while their contribution in polar media appears to be rather small. In the latter case, besides

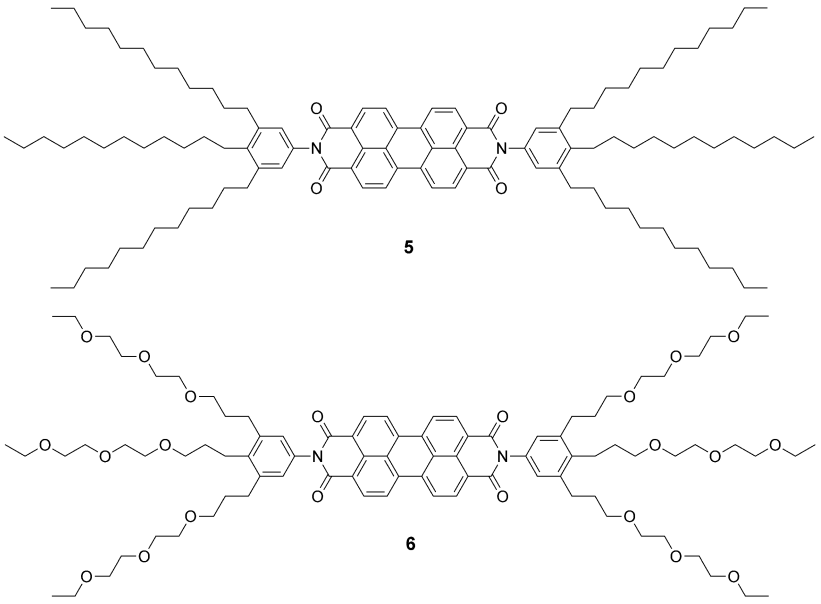

Figure 3. Chemical structures of PBIs **5** and **6**.

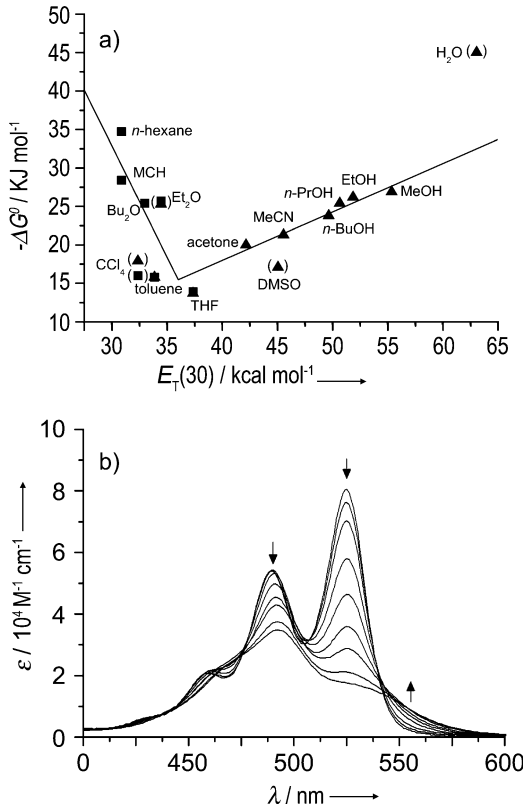

Figure 4. a) Plot of the standard Gibbs free energy $-\Delta G°$ for isodesmic aggregation versus solvent polarity $E_T(30)$ for PBI **5** (squares, $r = 0.98$) and PBI **6** (triangles, $r = 0.97$). The data points in parentheses (mainly for easily polarizable solvents, which undergo strong dispersion interactions with π surfaces) were not considered for the linear regression analysis. THF = tetrahydrofuran, DMSO = dimethylsulfoxide, MCH = methylcyclohexane. b) Concentration-dependent UV/Vis spectra of **6** in MeOH (6.1×10^{-7} M to 2.5×10^{-4} M) at 25 °C. The arrows indicate the spectral changes with increasing concentration.

dispersion interactions, hydrogen bonds play an important role, which is evident in the series of alcohols applied in these studies. It is remarkable that, upon changing to polar solvents, the increase in the $-\Delta G°$ value does not first take place in structured alcoholic solvents but already occurs in the dipolar aprotic solvents THF, acetone, and acetonitrile.

The significantly increased value of $-\Delta G°$ in water suggested the need for further investigations, first, because this value is given only as a lower limit[27] and, second, because it indicates a very strong hydrophobic effect. Indeed, the propensity of PBI **6** to undergo π–π stacking in water is so pronounced that essentially complete aggregation was observed with a binding constant of $K > 10^8\,\text{M}^{-1}$ and a standard Gibbs free energy of $-\Delta G° > 45\,\text{kJ mol}^{-1}$ even at nanomolar concentrations. This substantial increase in the $-\Delta G°$ value compared with all other values shown in Figure 4a provides proof of the large hydrophobic contribution of the solvent water. Although the significance of such hydrophobic effects is well known for many structure-creating processes in nature, such as, for example, protein folding, we are not aware of any further example from supramolecular chemistry for which such a comparably strong increase in the aggregation constant in water has been observed. In contrast, on the basis of solvent-dependent binding constants for the enclosure of pyrene in a hydrophobic cavity[31] and for the π–π stacking between 1,5-dialkylnaphthalenes and naphthalene diimides,[32] no special hydrophobic effect could be found.

The aggregation processes of PBIs **5** and **6** in the solvents depicted in Figure 4a can be followed by the spectral changes (Figure 4b) on transition from molecularly dissolved dyes to aggregated species upon increasing concentration. For non-aggregated PBIs, a clear vibronic fine structure of the electronic transition from the S_0 to S_1 state was always observed. This information disappears during the aggregation process because of strong excitonic interactions between the PBI chromophores,[33,34] and the ratio of the two most intensive absorption bands inverts. The spectrum becomes broader and unstructured with a reduced absorption coefficient. As a consequence of the hypsochromic shift of the dominant absorption bands of these aggregates, one can speak of H-aggregates (H denotes hypsochromic). Interestingly, PBIs with hydrophilic imide substituents form similar aggregate structures in water or methanol to those formed by PBIs substituted with nonpolar residues in organic solvents. On the basis of thermodynamic data (isodesmic aggregation) as well as changes in the absorption spectra upon aggregate formation and quantum chemical calculations, the structural model depicted in Figure 5 was developed, in which the individual PBIs in π–π stacks are rotationally displaced by about 30° to each other.[19,29] A further characteristic of this arrangement is the appearance of a long-lived, strongly red-shifted emission,[29] which could be attributed to a change in

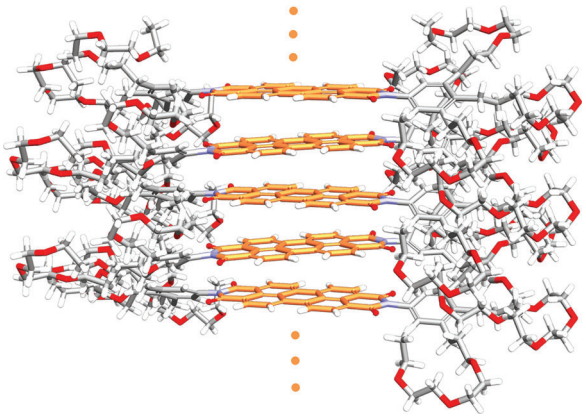

Figure 5. Schematic model for the columnar π-π stacking of PBIs in which alternating as well as helical segments may coexist. The average length of the π stack results from the thermodynamic parameters $\Delta H°$ and $\Delta S°$, as well as temperature and concentration.

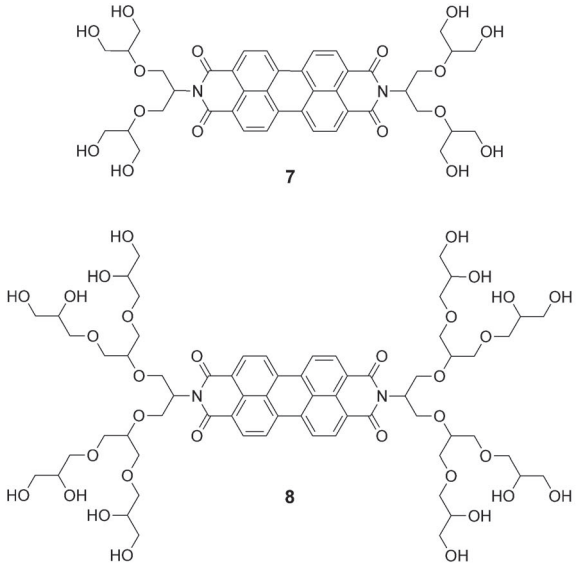

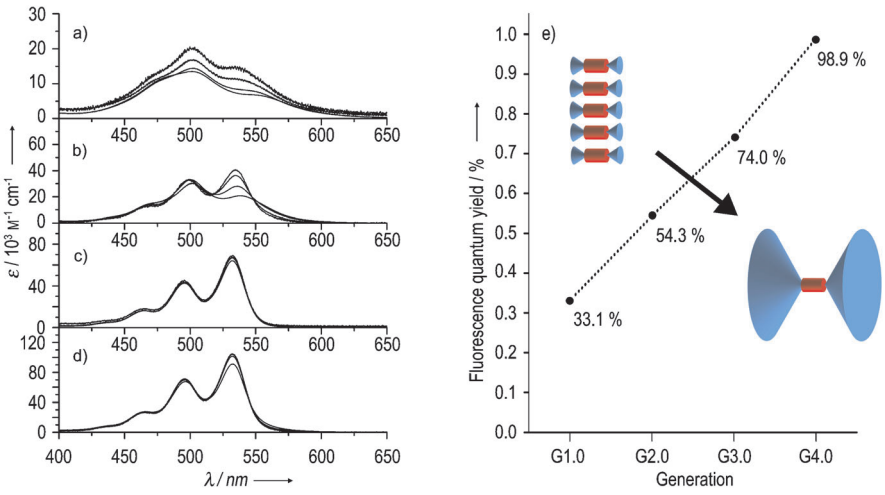

Figure 6. Chemical structures of **7** and **8** (above). a–d) UV/Vis absorption spectra of aqueous solutions of PBIs functionalized with polyglycerol dendrons of the 1st (a), 2nd (b), 3rd (3), and 4th (d) generation in a concentration range from 10^{-4} to 10^{-6} M. e) The effect of dendron substituents on the fluorescence quantum yield of the PBI chromophore at the highest accessible dilution (ca. 10^{-7} M). Reproduced from Ref. [37] with permission. Copyright (2010) RSC Publishing.

the supramolecular arrangement in the electronically excited state.[28b] An excited dimer (excimer),[35] which is comprised of two nearly parallelly oriented PBI building blocks, is generated within the dye stack through this relaxation process, and the long-lived emission of such dimers is attributed to a nearly forbidden optical transition (H-aggregate).[36]

Investigations on the aggregation propensities of dendron-functionalized perylene bisimides in water provided valuable information on the transition from molecularly dissolved dyes to aggregated species and its impact on the optical properties.[37] For this purpose, hydrophilic polyglycerol dendrons of generation 1 (G1) to 4 (G4) were attached to the imide nitrogen atoms of the PBI core and their optical properties and aggregation behavior in water were studied. UV/Vis studies revealed that G1-dendronized PBI **7** (Figure 6a) exists in an aggregated form over the whole accessible concentration range, as the G1 dendron at the imide position is apparently too small to sterically shield the PBI core and thus to suppress the aggregation.

In contrast, the transition from aggregated dyes to monomers is observable for the second generation dendronized PBI **8** once the solution is diluted (Figure 6b). The dendrons of the third and fourth generation are then sufficiently large to shield the π surfaces of the PBI effectively, thus the observed absorption spectra over the whole concentration range arise from PBI monomers. The degree of shielding is also reflected in the fluorescence quantum yields of this series of dendronized PBIs. As the size of the dendron increases, the fluorescence quantum yields of the PBIs increased from 33% for the first generation to nearly 100% for the fourth generation (Figure 6e). If the aggregation is suppressed effectively, PBIs can possess similarly high fluorescence quantum yields in water as in organic media. Substantial efforts are thus necessary to shield the chromophore in water because of the very strong propensity for π–π aggregation. UV/Vis studies with PBIs functionalized with oligoethylene glycol dendrons led to the same conclusion.[38]

The aggregation of PBIs can also be hindered by more simple approaches, such as the introduction of multiply charged ionic side chains, as the investigations with spermine-functionalized PBIs **9** and **10** have shown (Figure 7).[39] Thus, the bolaamphiphile **9** exists in a molecularly dissolved form in aqueous solu-

tion at low concentration and at a nearly neutral pH value. In the mostly protonated form, the positively charged side chains apparently hinder the π–π stacking through electrostatic repulsion. Accordingly, the fluorescence quantum yield for PBI **10** reaches a remarkable value of 90% in water. As the concentration of bolaamphiphile **9** in water is increased, however, aggregation takes place, which occurs together with an increase in the pH value to 4. This can be explained in such a manner that the protons of the side chains in the aggregate being transferred to the surrounding water to minimize the electrostatic repulsion. On the other hand, the hydrogen bonds between the positively charged ammonium groups and neutral amine groups of the side chains may facilitate the π–π stacking of PBIs. Upon increasing the distance between the protonated amine groups and the PBI core by the introduction of aliphatic spacer units (**10a**–**c**), the aggregation tendency of these PBIs is increased, and this is associated with a decrease in the fluorescence quantum yields. The hydrophobic interactions of these spacer units with each other result in the π–π stack being additionally stabilized, and hence the aggregation is favored. Atomic force microscopy (AFM) and TEM studies have shown that the PBI molecules are arranged into large rod-type structures, whose length and diameter increase as the spacer length increases (Figure 7).

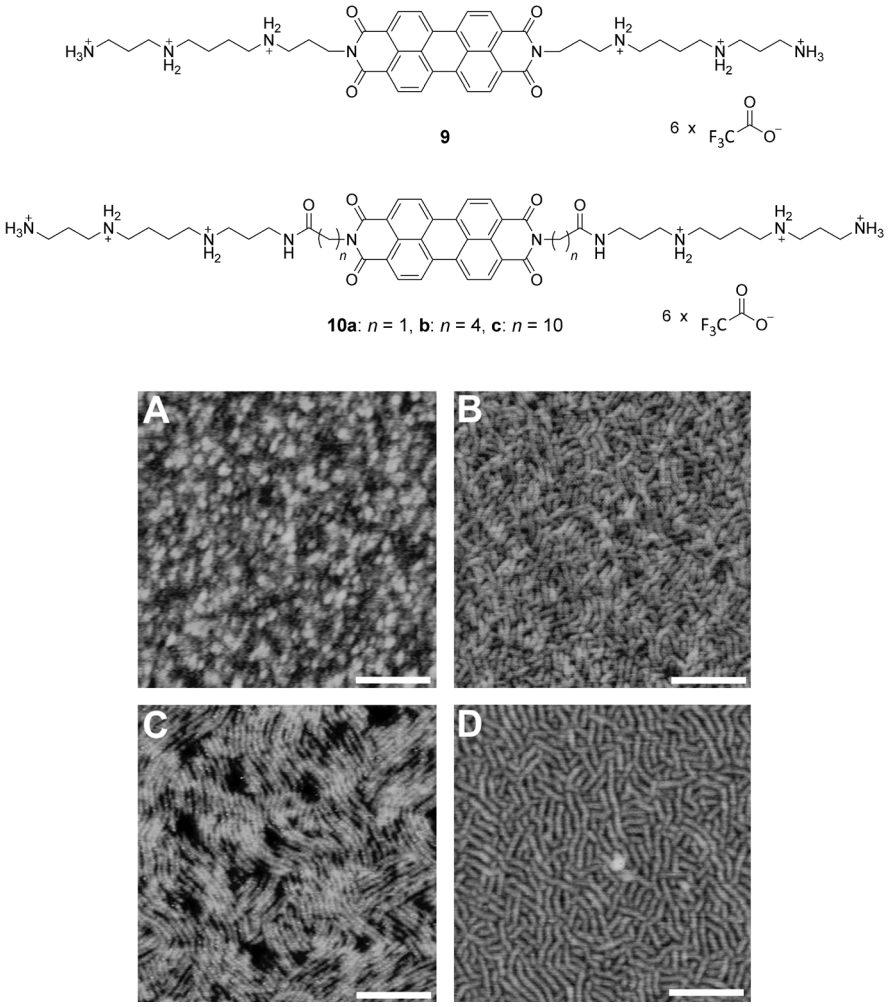

Figure 7. Chemical structures of spermine-functionalized bolaamphiphiles **9** and **10**, and AFM images of aqueous solutions ($c = 10^{-3}$ M) of **9** (A), **10a** (B), **10b** (C), and **10c** (D) that are spin-coated onto mica. The scale bar corresponds to 50 nm. Reproduced from Ref. [39] with permission.

Similar fluorescent rodlike nanostructures are also formed by the self-assembly of β-cyclodextrin-substituted PBI **11a** (Figure 8) in water.[40] The incorporation of a protonatable amino group in the vicinity of the PBI core facilitated an interesting pH-dependent control of the aggregation behavior. Thus, while the protonated form of **11b** creates only small aggregates, the deprotonated form assembles into larger flakelike structures.[41] Greater aggregates have also been reported for the crown ether functionalized PBI **12**.[42] Such aggregates could be easily separated with G4 glass filters, but, nevertheless, they appear to form dispersions in water that are stable for a prolonged time.

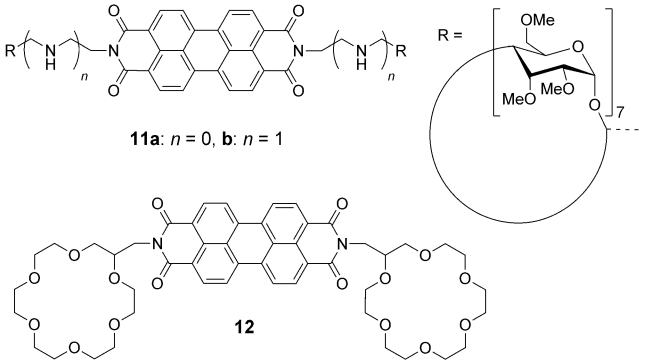

Figure 8. Chemical structures of PBIs **11a**,**b** substituted with β-cyclodextrin and that of PBI **12** substituted with a crown ether.

Another interesting class of water-soluble PBIs has been introduced by Hirsch and co-workers. The Newkome dendrons function in these PBIs as hydrophilic substituents at the imide positions and provide appreciable water solubility and also exert an aggregation-inhibiting effect because of their bulkiness and anionic character.[43] A bolaamphiphile bearing Newkome dendrons of the first generation again exhibited the typical characteristics of aggregated PBIs, that is, a broad absorption spectrum with a hypsochromically shifted absorption maximum and a weak fluorescence. The aromatic core in the symmetrical PBI **13** (Figure 9) containing second generation dendron substituents is, in contrast to the previous

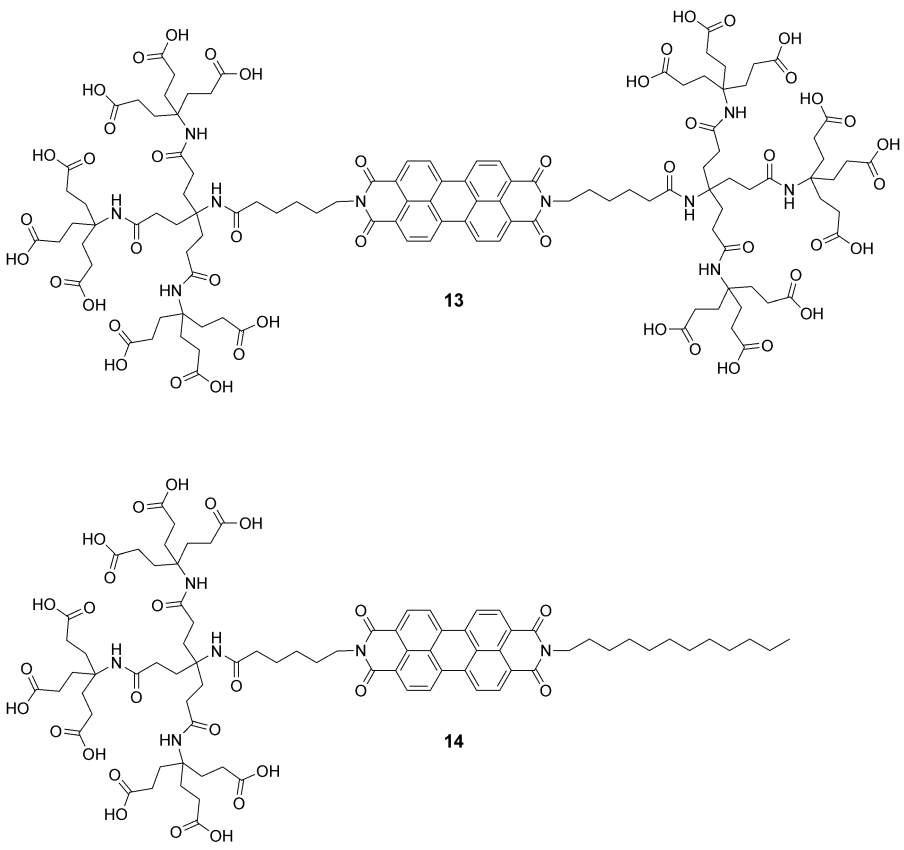

Figure 9. Chemical structures of PBIs **13** and **14** substituted with the Newkome dendron.

example, effectively shielded and thus is molecularly dissolved at lower concentration, which is reflected in an enhanced fluorescence of this PBI. This appears to be not only a consequence of the increased steric demand of the dendron units, but also a result of electrostatic repulsion, as most of the 18 carboxy groups are deprotonated at neutral pH. TEM investigations confirmed that the bolaamphiphile containing first generation Newkome dendrons is more prone to aggregation than the one with second generation dendrons. Accordingly, larger aggregates with irregular shapes were formed in the former case. Interestingly, defined aggregates can be obtained if one dendron substituent is replaced by a dodecyl chain, as in PBI **14**. The resultant amphiphile then self-assembles into spherical micelles in water, where the hydrophilic Newkome dendrons are turned outwards towards the surrounded aqueous medium and the alkyl chains form the hydrophobic interior core. In further studies, chiral alanine and lysine residues were incorporated between the PBI core and the Newkome dendron scaffold to increase the molecular order in the aggregates, and thus to achieve a diastereoselective self-assembly.[44]

3. Micelles, Vesicles, and Membranes by Self-Assembly of PBIs

A prediction of the supramolecular architectures that would be created by π–π stacking is challenging, particularly for those formed from amphiphilic building blocks in water where the hydrophobic effect exerts a decisive influence. The formation of different kinds of aggregate structures and their sizes are dependent on many factors, such as temperature,[45] concentration,[46] solvent composition,[47] molecular structure and the form of building blocks,[14a,30] steric interactions between molecular units and the presence of particular additives,[48] and the relative ratio of hydrophobic and hydrophilic units within the molecules.[9,49] In the case of block copolymers, the size of these supramolecular structures might also be influenced by the molecular weight of the polymer.[50]

As discussed in the previous section, substituents exercise a crucial influence on the ability of PBIs to aggregate in water. The effect of molecular shapes and the possibilities resulting from mixtures of differently shaped PBIs have been investigated by our research group only a few years ago.[30] It has been demonstrated with the amphiphilic, unsymmetrically substituted PBIs **15** and **16** that the morphology of the resultant aggregates can be predicted on the basis of the ratio of the hydrophilic and hydrophobic packing parameters[9] of the involved molecules (Figure 10).

The wedge-shaped amphiphile **15** bearing a hydrophobic hexylester chain at one end and a hydrophilic triethylene glycol chain at the other end assembles into micelles with a diameter of 4–6 nm, with the hydrophobic part forming the inner core, while the hydrophilic chains interacting with the surrounding water medium. However, coaggregation of **15** with dumbbell-shaped PBI **16** results in the formation of vesicles with a bilayer membrane. The combination of **15** and **16** in a 8:1 molar ratio in a H_2O/THF (2%) mixture leads to the formation of spherical structures with a diameter of nearly 100 nm and a membrane thickness of 7–8 nm. The latter value corresponds to approximately twice the length of the PBI monomers, and hence provides evidence for a bilayer membrane. Vesicles with larger or smaller diameters are formed upon increasing or decreasing the amount of **16**, respectively.[30] At a higher portion of **16**, the ratio of the hydrophobic part in the aggregate increases, which leads to an overall decrease of the surface curvature and ultimately to an enlargement of the vesicle. In the self-assembly of **15**, however, the curvature in the aggregate is at a maximum and the formation of considerably smaller micelles becomes feasible. The structures could be characterized by TEM, dynamic light scattering (DLS), and, because of their intensive fluorescence, also by confocal fluorescence microscopy.[30] The supramolecular structure of the obtained vesicles could be stabilized by photopolymerization of the terminal

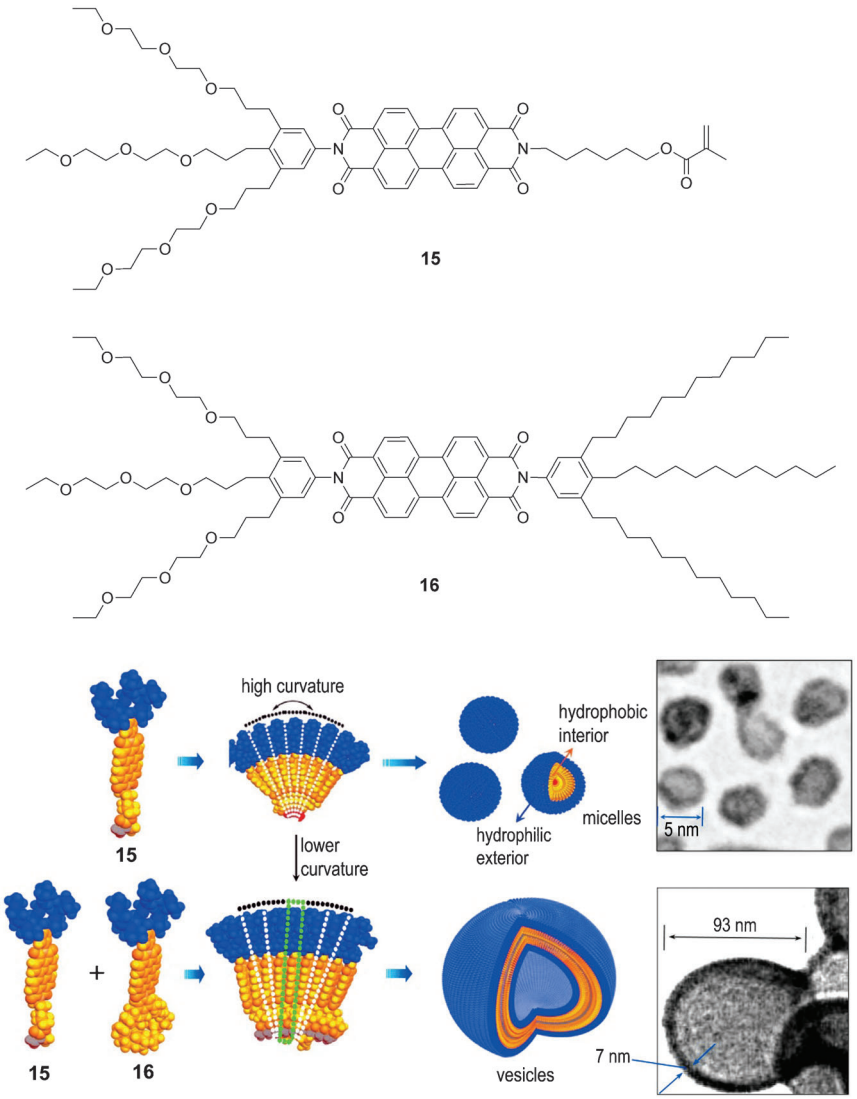

Figure 10. Chemical structures of amphiphilic PBIs **15** and **16** (top). Schematic representation of the formation of micelles by self-assembly of PBI **15** and of vesicles by coassembly of PBIs **15** and PBI **16** (bottom).

double bond in the hydrophobic side chain. Thus, the covalent linkage preserves the original aggregate structure and size, and enhances the morphological stability against external influences.

The preparation of vesicles based on amphiphilic perylene bisimides in an aqueous medium leads to the creation of a reaction compartment separated by a photoactive membrane. In further studies, these vesicles were loaded with water-soluble, protonatable bispyrene derivatives that upon photoexcitation with UV light under basic pH conditions undergo a fluorescence resonance energy transfer (FRET) to the PBI membrane, which functions as an acceptor (Figure 11).[51] This FRET process does not take place in acidic solutions, and thus the PBI membrane is not excited. The reason for this rests on the degree of protonation of the nitrogen atoms in the bispyrene derivative, which exists in a stretched conformation in acidic solution and in a stacked conformation in basic solution. While the stacked conformation exhibits a green excimer emission at 460–540 nm, the unstacked conformation emits blue light at 370–420 nm. Thus, the emission of bispyrene varies depending on the pH value. Under strong basic conditions (pH 11–13), the emission spectrum of the pyrene excimer overlaps nearly completely with the absorption spectrum of the perylene bisimide bilayer membrane, and thus the most efficient energy transfer from pyrene to the PBI membrane takes place under these conditions. As a result of this energy transfer, the membrane fluoresces upon photoexcitation of the pyrenes. The spectral position and band shape of the PBI emission emanating from the membrane are in accordance with the structural relaxation of excited PBIs with population of the excimer-type excited states, as discussed before for simple PBI stacks (Figure 5). The spectral overlap from the donor to the acceptor results in a pH-dependent fluorescence, which at pH 9 passes through the white light region, and is thus particularly interesting for diagnostic purposes (Figure 11).

A further amphiphile, PBI **17**, containing a galactosyl group as the hydrophilic unit has been reported by Faul and co-workers. This PBI forms right-handed superhelical structures with a diameter of 100 nm in a 1:1 mixture of water and THF (Figure 12).[52] These structures are composed of bundles of individual helical fibers, in which the galactosyl groups serve for the formation of highly ordered structures through hydrogen bonding.

Liu and co-workers have studied the aggregation behavior of the amphiphilic cyclodextrin–PBI conjugate **18**.[47a] Compared with the previously discussed bolaamphiphile **11**, PBI **18** exhibits a stronger aggregation capability because the π–π stacking of this PBI is more pronounced due to the absence of a second cyclodextrin unit and is additionally strengthened by the hydrophobic interaction of the alkyl chains. The morphology of the aggregates of PBI **18** is dependent on the solvent composition.[47a] TEM and SEM images obtained from a solution of **18** in pure methanol revealed the formation of nanorods, with the PBIs stacked on top of each other in a rotational manner[29] and the hydrophilic and hydrophobic residues pointing outwards in a rather random manner. The amphiphilic character of this PBI derivative becomes more evident in water-containing solutions. In contrast to the pure methanol solution, compact aggregates were formed in a 4:6 H_2O/MeOH mixture, with the hydrophobic alkyl chains avoiding the solvent and the cyclodextrin groups pointing outwards. The molecular arrangement becomes more defined at a higher water content (H_2O/MeOH = 9:1),

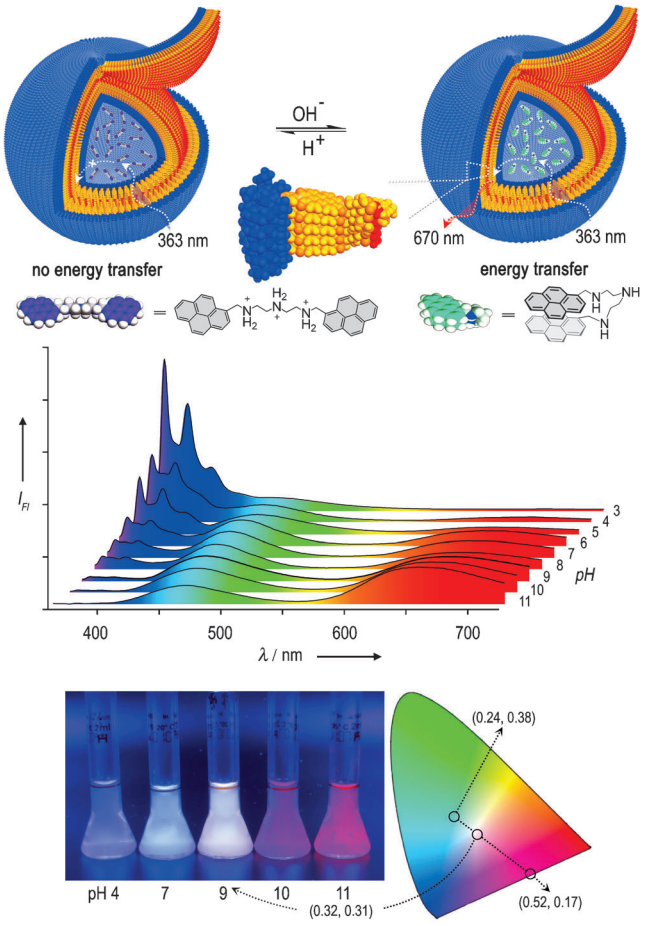

Figure 11. Schematic illustration of pH-dependent fluorescence resonance energy transfer in PBI vesicles loaded with pyrene donors (top), fluorescence spectra (middle), and a photograph of donor-loaded vesicles in aqueous solution at different pH values under UV light (366 nm), together with a CIE 1931 chromaticity diagram (bottom). Reproduced from Ref. [51] with permission. Copyright (2009) Nature Publishing Group.

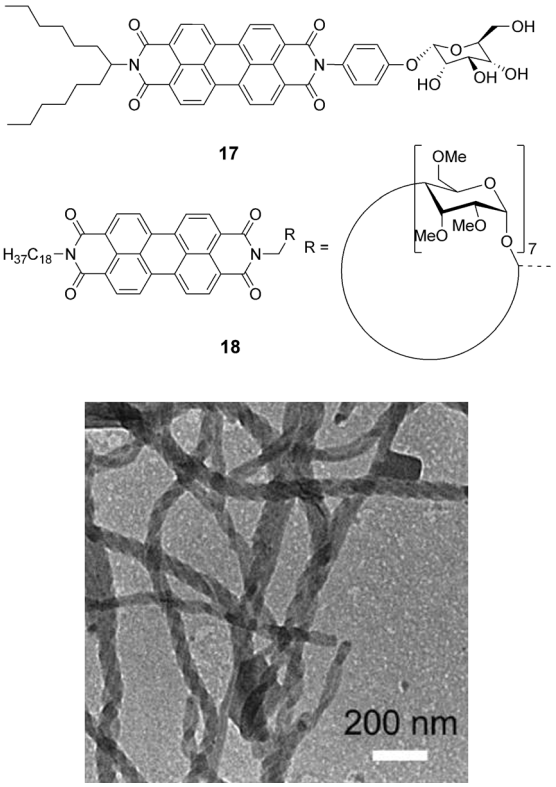

Figure 12. Chemical structures of amphiphilic PBIs **17** und **18** (top). Helical nanostructures in a TEM image obtained from a solution of **17** in a 1:1 mixture of water and THF (bottom). Reproduced from Ref. [52] with permission. Copyright (2011) RSC Publishing.

and for this solvent mixture the formation of vesicular structures was reported. These vesicles were embedded in a polyvinylidene fluoride (PVDF) membrane and used for the detection of organic amines in the gas phase by fluorescence quenching. These analytes could be bound to cyclodextrin units, thereby leading to a decrease in the excimer-type fluorescence of the PBIs. According to the authors, this fluorescence quenching is caused by two factors: the photoinduced electron transfer from amine analytes to the electron-poor PBI, and the inclusion of the analytes disturbing the well-defined aggregate structure and thus also the exciton migration in the aggregate. This also explains why PBI **18** is better suited for such an application than the bolaamphiphile **11**. The latter does not aggregate so strongly, and accordingly highly ordered, extended structures are not formed.

Likewise, symmetrically substituted PBI **19a** with trialkylammonium groups at the imide position has been introduced, with iodide as the counterions, for application as a sensor for amines (Figure 13). One-dimensional nanotubes were formed upon drop-casting of an aqueous solution of this PBI on a silicon substrate and slow evaporation of the solvent at room temperature. However, nanorods were formed from a solution of **19a** in methanol that did not have hollow interiors. Apparently, the application of different solvents results in different crystallization processes, since **19a** exists strongly aggregated in water and predominantly as monomers in methanol. Both nanostructures have been used for the detection of amines through electric conductivity measurements, and they showed high sensitivity particularly toward reducing agents that possess electron-donor groups such as hydrazine or phenylhydrazine. As a consequence of the larger surfaces, the hollow nanotubes obtained from aqueous solution are more effective for amine sensing than the rod-shaped aggregates obtained from methanol solution.[53] Moreover, this positively charged PBI has been used in thin films that were electrolytically self-assembled with negatively charged polyelectrolytes.[54]

In an interesting study, Tam-Chang et al. have investigated the structural effects of these (**19b**,**c**) and similar ionic PBIs (**20**, **21**) in regard to their lyotropic liquid-crystalline properties.[55] Despite containing different ammonium side chains and counterions, these PBIs exhibit similar aggregation behavior and optical properties in water. They form chromonic liquid-crystalline phases that are characterized by a transition from an isotropic to a nematic phase (N) and finally to a hexagonal phase (M) upon an increase in the concentration.[56] Accordingly, both **19b** and **20a** first form

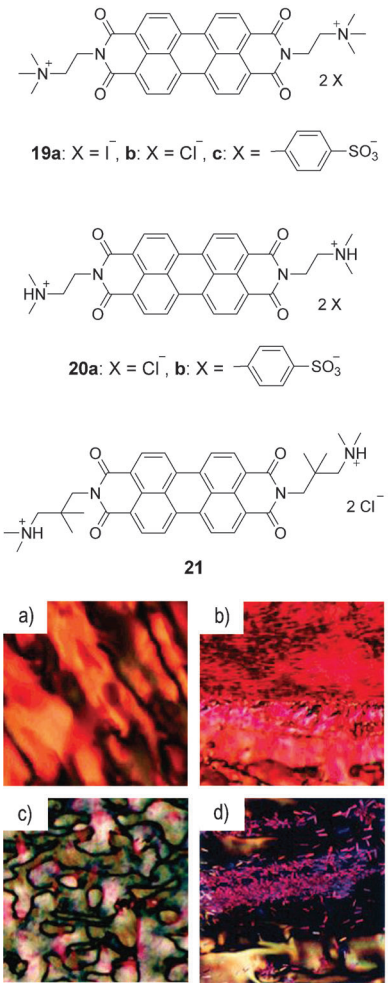

Figure 13. Chemical structures of ionic PBIs **19**, **20**, and **21** (top). Representative optical textures observed for different chromonic liquid-crystalline phases of PBIs **19b** und **21** in water. a) N phase of **19b** (6.8 wt%); b) granular M phase of **19b**; c) Schlieren texture for the N phase of **21** (18.8 wt%); d) crystals formed upon evaporation of the solvent from a solution of **21** in the N phase. Reproduced from Ref. [55a] with permission. Copyright (2008) American Chemical Society.

a nematic phase, while at higher concentrations they exhibit a hexagonal phase (Figure 13a,b). Protonation or methylation of the terminal amino groups clearly has only a minor effect on the phase properties, while the effect of counterions is more pronounced. Compared with the PBIs **19b** and **20a**, the transition from an isotropic to a nematic phase was observed only at a significantly higher concentration in the case of PBI **21**. A further increase in the concentration resulted in the formation of crystals, and not in a hexagonal phase (Figure 13c,d). Thus, the methyl groups between the PBI core and the ammonium units in **21** evoke a different packing behavior that reduces the range of the liquid-crystalline phase.

Rybtchinski and co-workers synthesized a series of amphiphilic PBIs possessing polyethylene glycol (PEG) chains at the bay positions (Figure 14), and investigated in detail their aggregation properties in aqueous media and also in the presence of particular additives.[57] Compound **22**, which is composed of two PBI units, forms nanofibers that are several micrometers long in a 4:1 mixture of water and THF.[58] The addition of the reducing agent sodium dithionite results in a dramatic color change of the aggregate solution in H_2O/THF (4:1) mixture from green to blue and a drastic drop in the viscosity. It is assumed that **22** is reduced up to the trianion and thus becomes significantly more soluble in the aqueous medium. As a consequence, the nanofibers dissolve and the micelles are now the dominant aggregate structures. This process is reversible, since the reduced system is oxidized by exposure to atmospheric oxygen which results in regeneration of the fiberlike aggregates. Recently published theoretical calculations have indeed shown that the dianion of a simple PBI is remarkably stable in water because of its aromaticity.[59] These findings are in agreement with the fact that perylene bisimides were initially developed not for their most popular application nowadays as red pigments, but rather as vat dyes.[60]

Unlike compound **22**, both PBI units in compound **23** are connected through a bipyridyl bridge. This molecule also assembles in aqueous media into uniform fiberlike structures, which through its three-dimensional supramolecular network forms an exceptionally stable hydrogel that can be heated to 70 °C for at least one hour without any apparent changes (Figure 15a,b).[61] Under reductive conditions, however, this gel changes to a fluid solution. Since this process is also reversible, the gel can be regenerated by exposure to atmospheric oxygen. More interestingly, the solvent can be removed quantitatively without affecting the structure of the ordered PBI fibers. Despite only noncovalent binding between the PBIs, the robust network resists external mechanical influences. Upon filtration of the aggregate solution, the authors isolated a porous supramolecular layer that can function as a membrane (Figure 15c–e).[62] This was demonstrated for the separation of gold nanoparticles in aqueous solution according to their size. Small gold nanoparticles with a maximum size of 5 nm could easily pass through the membrane, whereas larger particles were retained. Intriguingly, this membrane can be recycled by dissolving it in organic solvents and reinitiating the self-assembly process by the addition of water.

PBI **24** has a terpyridine unit in the bay position as an anchor functionality, which can coordinate soft transition-metal cations. Thus, this molecule arranges differently in the presence of different metal cations, and diverse morphologies can be observed.[63] PBI **24** alone forms in aqueous media long fiberlike structures, which are comprised of individual segments arranged in sequence, and in these structures only the PEG chains are turned towards the water. Upon binding the metal cation Pd^{2+}, this PBI also forms long, fiberlike structures, but they possess tubular architectures. The hollow interior is covered by the receptor units, whose cationic Pd centers constitute the interior surface. Upon binding the Ag^{+} cation, PBI **24** assembles preferentially into two-dimensional aggregates.

In the presence of platinum cations, PBI **24** creates predominantly vesicular aggregates with a bilayer membrane, and Pt-Pt interactions between two neighboring complexes

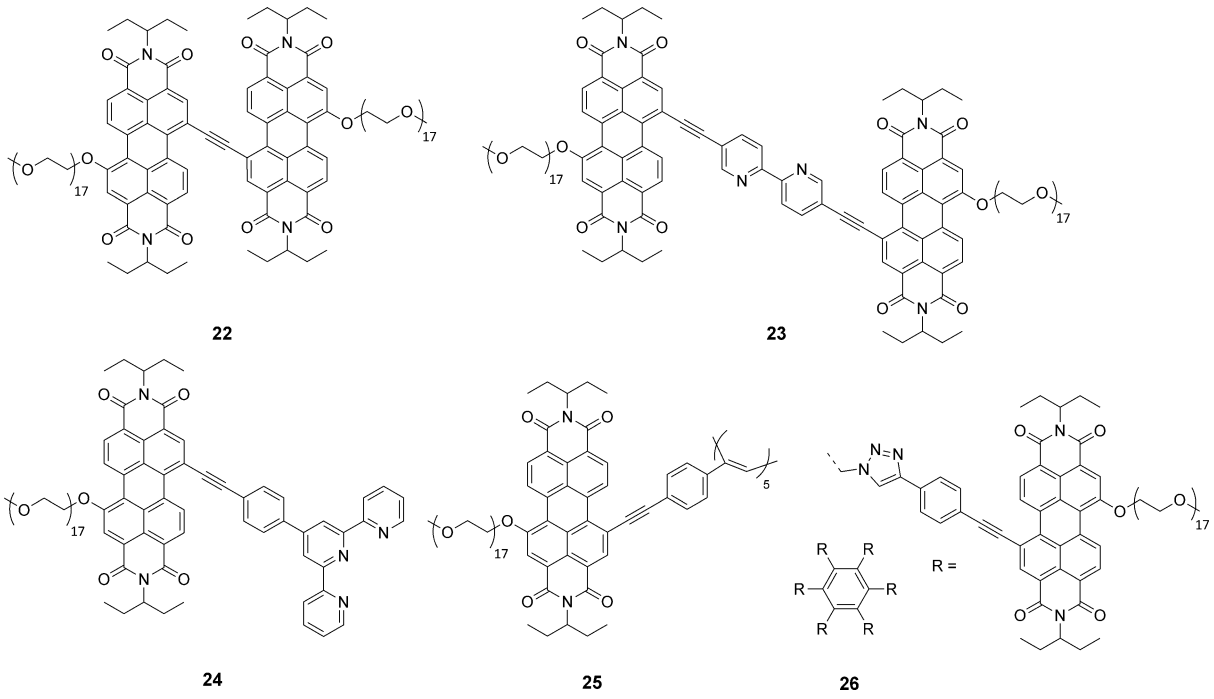

Figure 14. Chemical structures of PBIs **22**–**26** substituted at the bay position with PEG.

possibly contribute to their formation.[63] Moreover, tripeptide frameworks containing a terminal cysteine residue could be connected with this PBI through the thiol group of cysteine, which binds to the coordinated platinum center.[64] Kinetic intermediates in the self-assembly of these complexes in aqueous media could be detected by spectroscopic and electron microscopy methods. The formation of equilibrated supramolecular structures is thus simply delayed in the presence of the strong hydrophobic interactions of PBIs in water. The structural motif described here could also be incorporated into PBI oligomers. PBI pentamer **25** forms a two-dimensional porous network in aqueous solution,[65] while PBI hexamer **26** assembles into tubular structures in a water/THF (7:3) mixture that show confinement of the exciton and thus localized emission. A high binding constant of about $10^9\,\text{M}^{-1}$ was reported for the aggregation of PBI **26**,[66] which is consistent with the thermodynamic data described at the beginning for PBI **6**.

4. π–π Stacking of PBIs in and with DNA

The outstanding fluorescence and electron-acceptor properties of PBIs appear to be particularly interesting for a diagnostic application based on intercalation into ribonucleic acid (RNA) or deoxyribonucleic acid (DNA). Thus, we devote a separate section to this subject, in which we highlight the potential of PBIs for studying biomolecules, particularly DNA, and their physiological functions on the basis of altered absorption properties, fluorescence signals, or electronic properties. In principle, there are two different possibilities by which PBIs can interact with DNA. On the one hand, these chromophores can be a part of DNA–PBI conjugates once they are covalently connected to oligonucleotides and, on the other hand, they may interact with DNA bases through noncovalent π–π interactions (upon intercalation).

It has been known for long time that water-soluble PBIs undergo π-stacking interactions with DNA bases. Cationic PBIs, in particular, showed enormous potential for the stabilization of DNA G-quartets, which are guanine-rich (G-rich) secondary structures of DNA that can be found mainly at the end of chromosomes, that is, in telomeres; the latter play important roles in cell division and DNA replication.[67] Telomeres are comprised of tandemly repeated units of the G-rich base sequence TTAGGG, and may extend up to 25000 base pairs. This hexanucleotide sequence at the end of linear chromosomes ensures complete replication of chromosomal DNA and also protects the chromosomes against fusion and degradation. Although most of the telomeric DNA structures are double-stranded, there are also noncanonical base pairs such as four-stranded G-quadruplexes, in which the four guanine bases form a planar surface through Hoogsteen interactions.[68] Since erosion of telomeres takes place over time and they become progressively shorter after every cell division, an enzyme system has evolved that biocatalytically restores the telomere length. The decisive enzyme in this process is the telomerase, a reverse transcriptase, which first has to unwind the G-quartet structures so that the telomere can be subsequently extended. Since the telomerase exhibits especially high activities and is over-expressed in cancer cells, appreciable efforts have been made to inhibit this enzyme in order to develop an approach for cancer therapy. It has been shown that extended π-conjugated molecules can stabilize the G-quartets to such an extent that they can no longer be unwound, and as a result the telomerase activity is inhibited.[69,70]

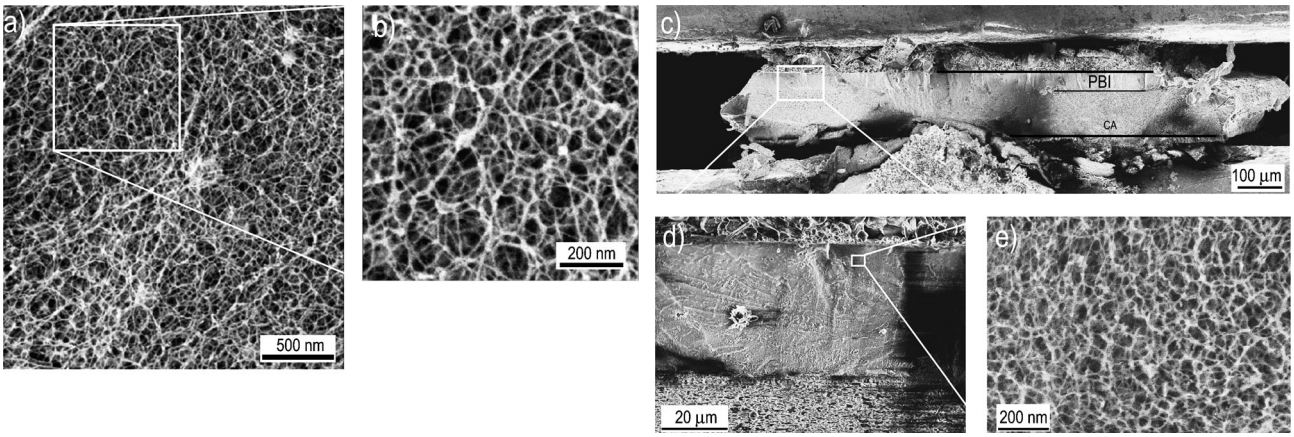

Figure 15. a) Cryo-SEM image of a sample prepared from a solution of aggregated **23** (10^{-4} M) in a 4:1 mixture of water and THF. b) Magnification of the framed area in (a). Reproduced from Ref. [61] with permission. Copyright (2009) American Chemical Society. c) Cross-section of a 1×1 mm^2 area of the supramolecular membrane (0.65 mg **23** per cm^2) on a cellulose acetate (CA) support. d) Magnification of an area in (c), showing the border between the rough CA layer and smooth PBI membrane. e) High magnification of the PBI membrane. Reproduced from Ref. [62] with permission. Copyright (2011) Nature Publishing Group.

Compound **27** is possibly the best studied PBI derivative in terms of G-quartet–PBI interactions (Figure 16). This compound contains two piperidine substituents at the imide positions, and is thus generally denoted as PIPER in the literature.[71–74] The protonation of the amine nitrogen atoms under neutral conditions ensures water solubility and strengthens the binding between the chromophore and tetrameric, parallel G-quadruplex DNA—which is otherwise enabled through π-π interactions—by electrostatic interactions of the positively charged ammonium side chains with the negatively charged phosphate backbone of DNA.[71] Moreover, PBI **27** initiates the formation of G-quartets from DNA oligomers that contain two tandem repeats of TTAGGG sequences.[72] PBI **27** can also effect the transition of duplex DNA, which is paired through Watson–Crick hydrogen bonding, into G-quadruplex DNA.[73] Studies with the enzyme helicase Sgs1, which preferentially unwinds G-quadruplex DNA but also duplex DNA to a small extent, have impressively demonstrated the selectivity of the binding of PBI **27** to DNA.[74] Thus, it was shown that the nearly exclusive binding of **27** to G-quadruplex DNA prevents its unwinding by this enzyme, while duplex DNA can still be enzymatically unwound because of the lack of stabilization by this PBI. In parallel to the increasing tendency of **27** to aggregate upon changing from acidic to basic conditions—protonation under acidic conditions counteracts the aggregation (see Section 3)—the binding selectivity also increases. For example, the selectivity of **27** for G-quadruplex DNA over duplex DNA is higher at pH 8.5 than at a neutral pH value.[75]

By considering these interesting properties, it is not surprising that a large number of PBIs with various substituents at the imide position have been investigated in regard to their interaction with G-quartets. Figure 16 depicts a small selection of such PBIs, which will be discussed in detail in the following. PBIs with basic residues or cationic side chains (**27**, **28**) have been shown to be best suited for such studies.[76] Neutral PBIs such as **29** also stabilize G-quartets, but with comparably lower affinity,[77] while negatively charged PBIs barely bind,[76b] thus convincingly demonstrating the crucial influence of ionic interactions with DNA backbone. The binding affinity can still be increased if the PBI contains special DNA groove binding units as substituents such as, for example, in PBI **30**.[78] PBIs substituted at the bay positions, whereby the optical properties of the formed complexes can be varied, have also been investigated.[79] G-quartets may also be created if PBI is terminally connected with a guanine-rich DNA strand at its imide position. The strong π–π interactions between terminal PBIs and DNA bases drive the association of guanine strands, and thus a tetrameric, parallel G-quartet is preferentially formed.[80] Since all aspects of this topic, such as, for example, the selectivity of PBIs for particular topologies of G-quartets and selectivity compared to duplex DNA, could not be covered here extensively, we refer the interested reader to further literature.[70]

It has also been known for a long time that the use of PBIs as linker units in DNA hairpin constructs can also stabilize rather unusual DNA secondary structures such as DNA triplexes through hydrophobic interactions with the neighboring DNA bases. Thus, it was shown that a target DNA single strand can be bound to two DNA strands that are connected by a PBI linker and are complementary to the target single strand, thereby leading to a hairpin DNA triplex structure.[81] Watson–Crick base pairing with one strand and Hoogsteen base pairing[68] with the other strand contribute to the stabilization of the triplex. But what effect does the covalent incorporation of the PBI chromophore into DNA sequences actually have? To answer this query, numerous DNA–PBI conjugates, in which PBIs were covalently linked to oligonucleotides, were synthesized in the last few years and their properties were thoroughly investigated. These studies are discussed in the following.

It was soon shown that DNA–PBI conjugates that are constructed by the incorporation of single-stranded DNA sequences at the imide positions of PBIs can hybridize with complementary DNA–PBI analogues.[82,83] The resulting

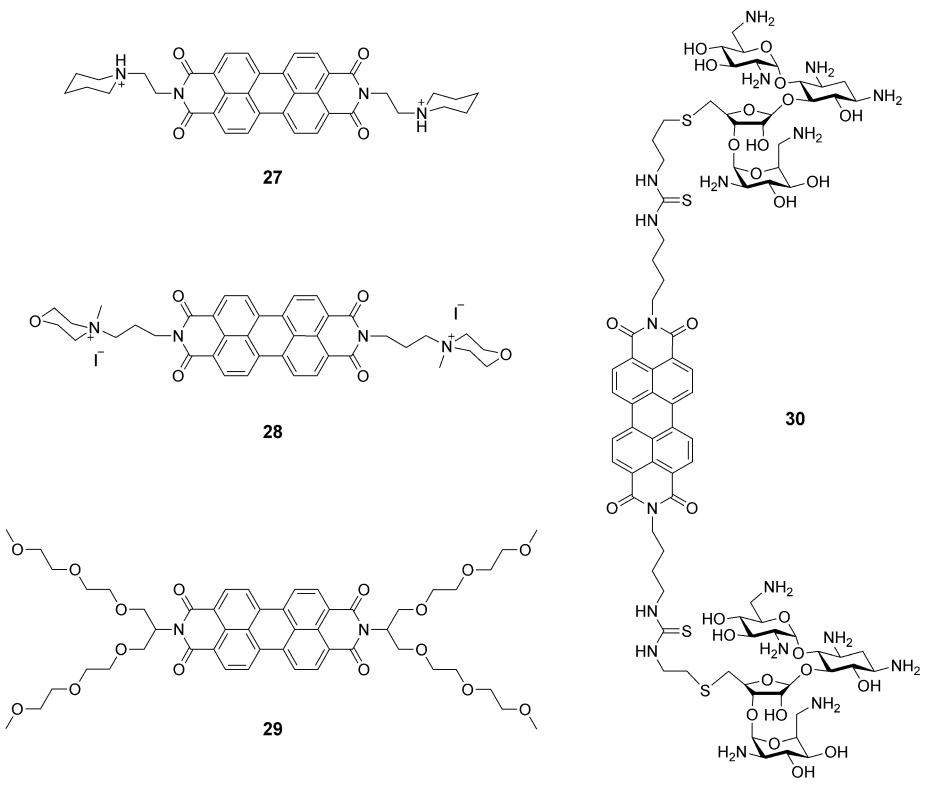

Figure 16. Chemical structures of the G-quartet-binding PBIs **27**–**30**.

duplex DNAs show enhanced stability because, besides hydrogen bonding between DNA bases, the π–π interactions between the PBIs located opposite to each other in the duplex DNA also contribute to the stability.[82] The effects of the incorporation of such PBIs in single-stranded DNA on aggregation were studied first with a DNA–PBI oligomer, in which the PBI chromophores stack depending on temperature.[84] No interaction between the PBI units of the polynucleotide shown in Figure 17 (DNA **1**) was observed at room temperature. Apparently, the DNA sequences prevent such an interaction through their steric and anionic properties. Heating this conjugate, however, resulted in the π–π stacking of PBIs, and led to the folding of this polynucleotide. Since this folding process should principally be disfavored at a higher temperature because of the loss of conformation entropy, a strong entropy-driven hydrophobic effect is apparently involved, which leads to the aggregation at higher temperature.

In a much larger number of studies, PBIs were incorporated in double-stranded DNA and their function as a base-pair surrogate elucidated. The molecular size of a PBI corresponds nearly to that of a base pair, and thus it should also exhibit a similarly strong π–π interaction with neighboring base pairs in DNA. Figure 18 depicts a model for the π stacking of a 5′-terminally attached PBI chromophore with a double-stranded DNA. To realize such an interaction in an internal position, a base-free 2′-deoxyribofuranoside needs to be incorporated at a respective position in the opposite strand. In this case, the emission of the PBI is rather weak because of π–π interactions or photoinduced electron-transfer process with the adjacent DNA bases. Temperature-dependent fluorescence spectra showed that the PBI emission is only moderately increased even after dehybridization (Figure 19) and the

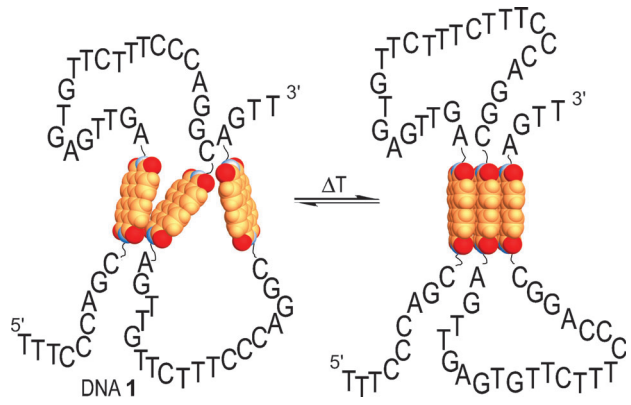

Figure 17. Thermophilic properties of the DNA–PBI trimer DNA **1**.

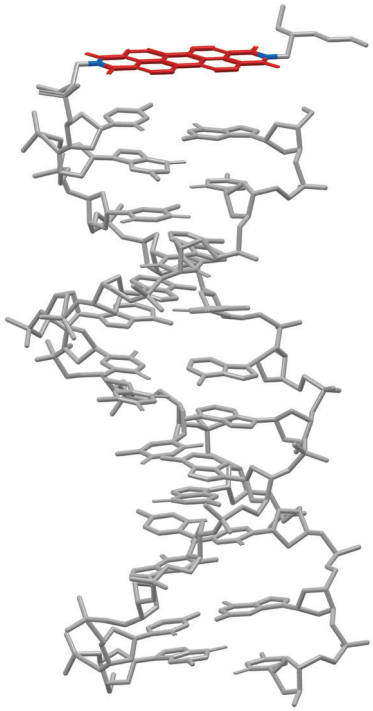

Figure 18. Model for the π-π stacking of a PBI chromophore (red) attached to the terminal position of a duplex DNA with the adjacent DNA bases.

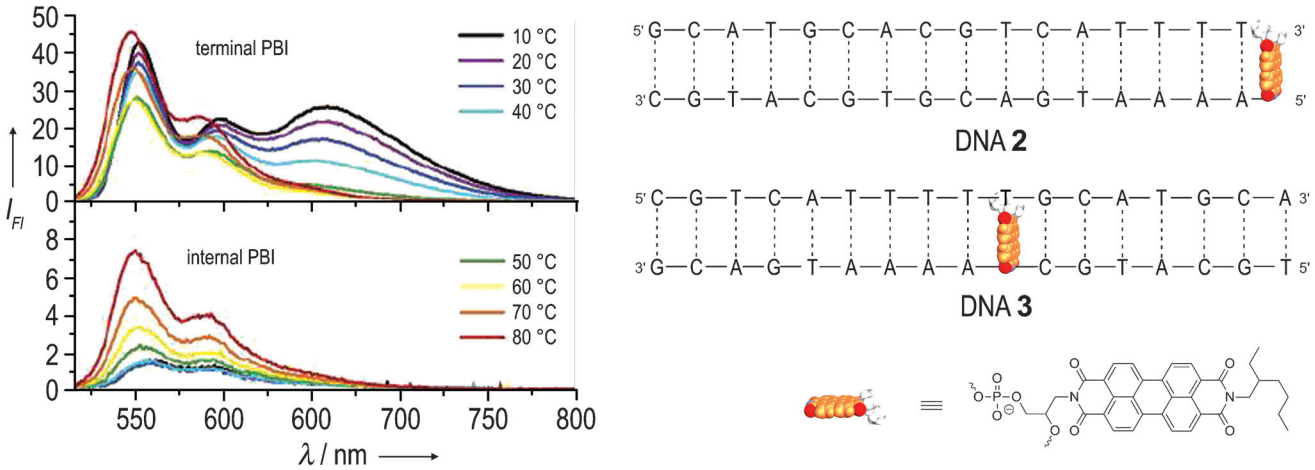

Figure 19. Schematic representation of PBI–DNA conjugates with terminal (DNA **2**) and internal PBI chromophore (DNA **3**), and the respective temperature-dependent fluorescence spectra (2.5 μM DNA in 10 mM sodium phosphate buffer, pH 7, $\lambda_{ex} = 505$ nm). Reproduced from Ref. [85] with permission. Copyright (2006) American Chemical Society.

absorption spectra exhibit only a slight hyposochromic shift of the absorption maximum upon dehybridization.[85] The observed weak emission indicates a quenching of the fluorescence by an electron-transfer process from the electron-rich DNA bases to the electron-poor PBI.[86]

Intensively fluorescent DNA–PBI conjugates can, however, be constructed if the interaction of the PBI with itself or with the adjacent base pairs is suppressed. This was achieved by the introduction of "isolator" molecules that do not possess any π electrons and shield the chromophore from neighboring π systems.[87] A second approach is based on the introduction of electron-donating substituents in the bay positions of the PBIs. As a consequence of an electron-rich aromatic core, as in the case of *N*-pyrrolidinyl-substituted PBI for example, a quenching effect by adjacent guanine bases no longer occurs.[88]

If the PBI is terminally attached to a duplex DNA, as in DNA **2** (Figure 19, right), an excimer-type emission is observed, which suggests a dimerization of two PBI–DNA strands through aggregation of the terminal PBIs.[89] Interestingly, the formation of the PBI dimer aggregate is no longer possible after dehybridization, which is expressed by a monomer-like PBI emission. A completely intact DNA secondary structure is thus a prerequisite for excimer formation. This motif was used in subsequent studies to construct supramolecular DNA structures which are arranged in a defined way through strong π–π interactions between terminally attached PBIs. The "three-armed" duplex DNA–PBI conjugate DNA **4** (Figure 20) thus aggregates spontaneously above a critical concentration.[90]

PBI stacking is also possible if this chromophore functions as a linker unit in a DNA hairpin (e.g. DNA **5**) or in a dumbbell-shaped DNA construct (e.g. DNA **7**; Figure 20). Lewis and co-workers synthesized a series of such PBI–DNA hairpins[82,91] and showed that PBI units do not interact with each other in buffered aqueous solution, but instead form stable π–π stacks with the adjacent base pairs (DNA **5**). The interaction with neighboring AT bases pair leads to fluorescence quenching, and thus the PBIs fluoresce only very weakly in these conjugates. However, in the presence of an excess amount of sodium chloride such DNA hairpins assemble into dimers (DNA **6**) through PBI–PBI interactions. This effect is, amongst other things, due to the fact that the higher salt concentration enhances the hydrophobic effect of

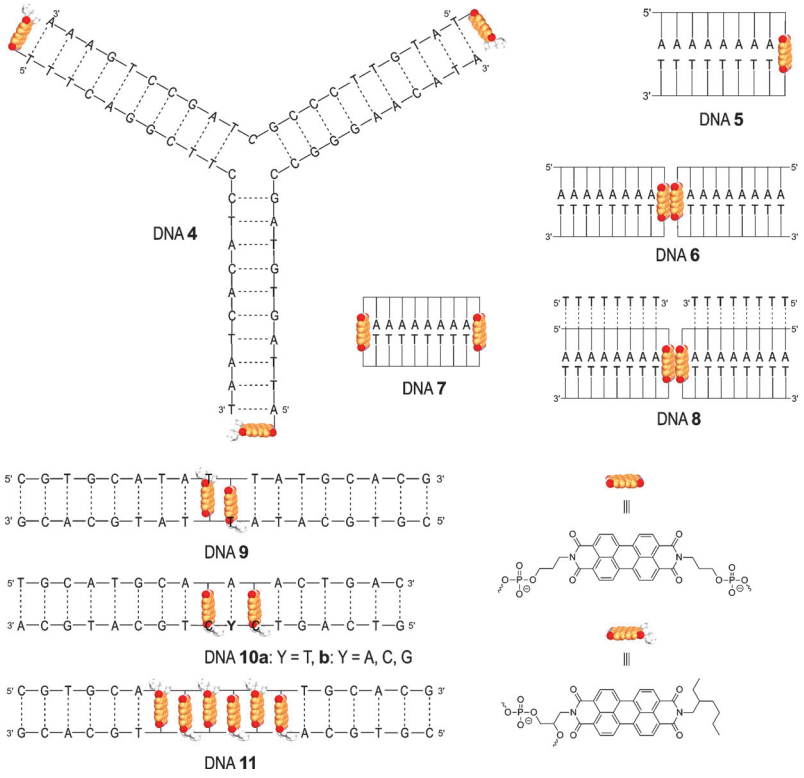

Figure 20. Schematic representation of different PBI–DNA conjugates (DNA **4**–**11**).

the PBI surfaces and thereby leads to stacking. The PBI–PBI interaction is then so strong that it can only be broken by increasing the temperature until the double-stranded DNA melts. In contrast, the dissociation of the dimer occurs prior to dehybridization at a lower salt concentration. On the basis of these results it was concluded that an intact secondary structure at a sufficiently high salt concentration is a prerequisite for the formation of a stable dimer from two PBI–DNA hairpins.[91a] A similar behavior was observed for the dumbbell-shaped PBI–DNA conjugate DNA **7**, which first exhibits a monomeric PBI absorption spectrum in buffered aqueous solution, but the appearance of the spectrum corresponding to PBI dimer aggregates was observed at sufficiently high salt concentration, thus suggesting formation of supramolecular polymers. Indeed, AFM and TEM images showed branched fibers composed of seven hexagonally arranged double-stranded DNA polymers.[92] However, if these DNA structures are dehybridized, the PBI units stack intramolecularly, and thus structurally defined, extended aggregates are no longer accessible.[93] Investigations of the excited state, charge transfer, and spin dynamics were performed on DNA hairpins in which a GC base pair was incorporated and its distance to the PBI linker was systematically enlarged.[94] These DNA hairpin structures also led to stabilization of DNA triplexes (e.g. DNA **8**). Thus, different triplexes could be produced by binding poly(dT) single strands to PBI hairpin structures consisting of poly(dT) and poly(dA) strands.[95]

π–π interactions between PBIs placed in an internal position of double-stranded DNA can be observed if they are located in the direct neighborhood in the same single strand or opposite to each other in the double helix (Figure 20). In the latter case (DNA **9**), the PBIs exhibit strong electronic interaction leading to excimer fluorescence, which changes to a typical monomer fluorescence upon dehybridization of the duplex DNA into the complementary single strands.[89] This behavior was used only recently in a DNA probe, in which two PBIs were positioned in a hairpin opposite to each other, thus enabling electronic coupling with each other. The addition of a complementary DNA single strand results in the separation of the PBI dimer, and hence the hybridization with the target DNA can be proven by the appearance of monomer-type PBI fluorescence.[96] Higher melting temperatures of DNA–PBI conjugates compared with those of their analogues without PBIs reveal that the hydrophobic PBI interactions stabilize DNA double strands.[89,97] The driving force for the formation of the intrastrand dimer is so pronounced that the PBIs can only be isolated from each other if they are separated by a matched DNA base pair, for example, AT in DNA **10a**. In the case of a single-mismatched base pair, for example, AA in DNA **10b**, which results in a weaker interaction of the DNA bases, the base pair is already squeezed out from the strand by both PBIs, and thus excimer fluorescence reappears.[89] It was shown that such PBI–DNA strands can clearly differentiate between a complementary and noncomplementary counterstrand. The amount of the complementary strand could be assessed on this basis even in mixtures of both counterstrands.[89] If a base pair is placed between two PBI chromophores located on opposite strands, this base pair can also be squeezed out from the DNA strand as a result of the strong PBI interaction. An AT base pair, which possesses two hydrogen bonds, is already separated at room temperature, while this happens only at higher temperature in the case of a GC base pair with three hydrogen bonds.[98]

No further stabilization of the DNA could be achieved by incorporation of a π stack with multiple PBI units in the duplex DNA. As Wagenknecht and co-workers noticed, the DNA double helix tolerates the formation of a dimer, but loses its stability by the presence of several PBIs that interact with each other, which was shown with a DNA strand containing six diagonally interacting PBIs (DNA **11**).[97] In this case, the PBIs are arranged in an alternating stacked fashion, like in a zipper. Here, the excimer fluorescence, however, cannot be changed to the monomer-type fluorescence by melting the DNA because a strong π–π interaction between the three adjacent PBIs still exists.

Another approach for the detection of single-stranded DNA was developed by Häner and co-workers that was based on the interaction of the electron-rich pyrene chromophore with the PBI chromophore in duplex DNA to give a stable donor–acceptor complex.[99] As a result of this interaction, the fluorescence of the PBI and pyrene was nearly completely quenched.[100] When both chromophores are components of a DNA hairpin (DNA **12**), a highly stable aggregate structure with a pyrene-PBI-pyrene-PBI sequence is thus achieved. If the PBIs and pyrenes are separated from each other upon hybridization with a DNA counterstrand, then the excimer

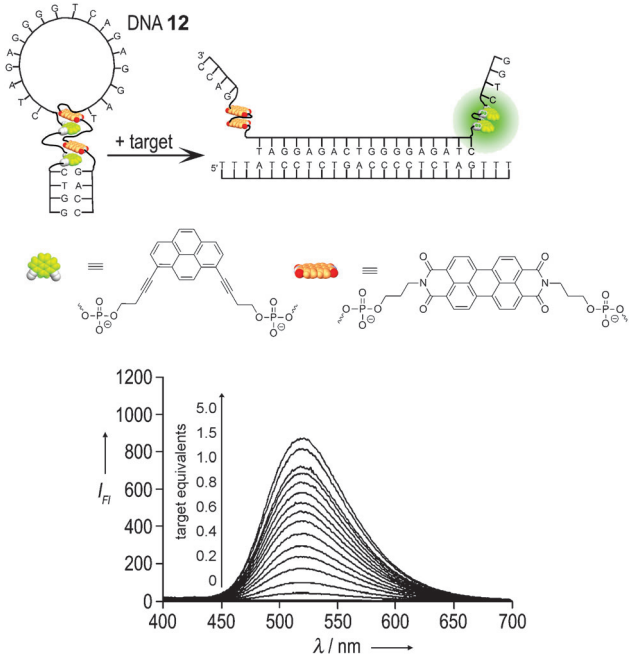

Figure 21. Top: Schematic illustration of the operating mode of a PBI-pyrene-functionalized hairpin as a DNA probe. Hybridization with a target DNA separates the PBI and pyrene units from their non-fluorescent donor–acceptor complex with formation of an emitting pyrene excimer. Bottom: Fluorescence readout by the hybridization of DNA **12** with a complementary target DNA (λ_{ex} = 370 nm, 10 mM phosphate buffer, pH 7.0, 100 mM NaCl, 37 °C). Reproduced from Ref. [99b] with permission.

formation between the pyrenes results in an intensive fluorescence, and thus the binding to the counterstrand can be detected (Figure 21).

In this section we have discussed how PBIs that are bound to nucleic acid sequences interact with themselves or with (pseudo) base pairs of DNA through π–π interactions. For a general overview on the arrangement of chromophores in DNA–dye conjugates we refer to a review recently published by Häner and co-workers.[101]

5. π–π Stacking between PBIs and Functional Carbon Materials

In addition to the interaction of PBI dyes with DNA and the resulting potential applications, particularly in the area of medicine, water-soluble PBIs should also be able to undergo π-stacking interactions with other π systems as a result of their previously discussed properties. Indeed, a nice example of this ability was recently shown by Hirsch and co-workers on using their PBIs substituted with the Newkome dendron (Figure 22).[102] These PBIs are well-suited for the dispersion of poorly soluble extended π-conjugated carbon materials such as single-wall carbon nanotubes (SWCNTs) or graphenes. The basis for this is a strong π–π interaction between the electron-poor PBI derivative and the π surface of the carbon materials. The interaction of SWCNTs with the water-soluble PBI amphiphile **13** led to the dispersion of carbon nanotubes, and isolated individual nanotubes could also be generated. The fluorescence of PBIs is quenched when they adsorb onto the surface of the nanotubes. Spectroscopic investigations revealed that a pronounced electronic coupling between the carbon nanotube and PBI occurs, which should lead to photoinduced charge-transfer processes.[102–104]

The dispersion and isolation of individual carbon nanotubes, which are already noticeable at a PBI concentration of 0.004 wt %,[102] can be followed by the fluorescence of the nanotubes, which is, however, weaker than when conventional detergents such as sodium dodecylbenzenesulfonate (SDBS)

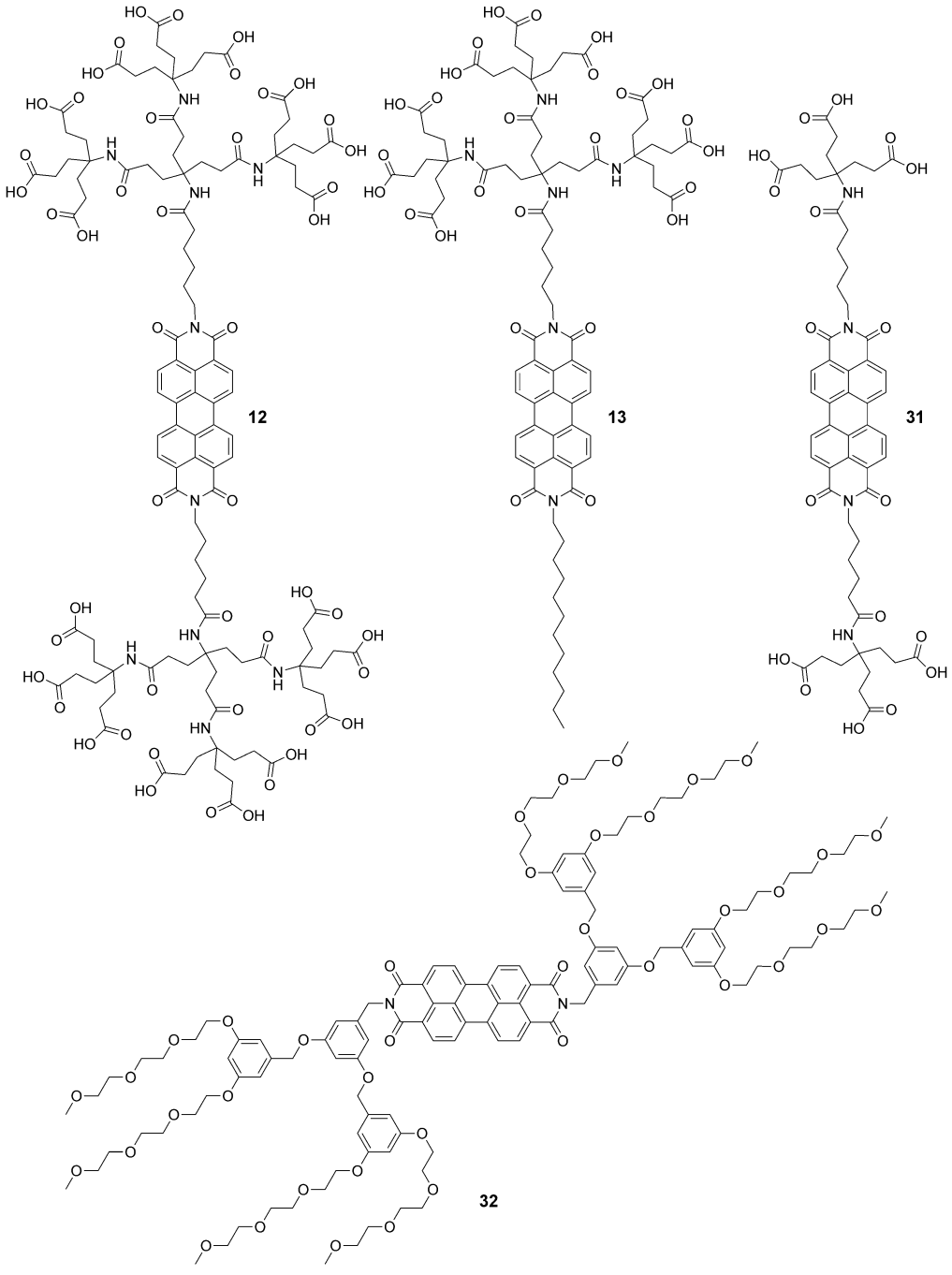

Figure 22. Chemical structures of Newkome- (**12**, **13**, **31**) und OEG-dendronized (**32**) PBIs, which were used for the dispersion of functional carbon materials. The structures of **12** and **13** are shown here again for a better overview.

are used instead of a PBI. Investigations with a first generation bolaamphiphile (PBI **31**) showed that carbon nanotubes can play the rather unusual role of an electron donor as a consequence of the interaction with the strong PBI electron acceptor, and thus a radical ion pair can be formed by photoinduced electron transfer.[103,104] It could be shown by comparing the near infrared (NIR) fluorescence of nanorods that different PBIs interact differently with nanorods. While PBI **12** quenches the NIR fluorescence of nanorods completely, it is still clearly observable for the interaction with PBI **13**. This shows that the interaction of PBIs with SWCNTs is dependent on the structural features of the PBIs and presumably relates to their propensity for self-assembly (see Section 3). The pH value of the buffer solution used also has a significant influence on the ability of PBI **12** to disperse carbon nanotubes. This ability is more pronounced at higher pH values because of the Coulombic repulsion of the negatively charged carboxylate groups of the PBIs (Figure 23).[105] It should also be mentioned that PBI **12** was successfully used for the dispersion of graphene sheets, thus emphasizing the potential of water-soluble PBIs as surfactants for the dispersion of carbon materials. In this way, multilayer stacks could also be separated from graphite.[106]

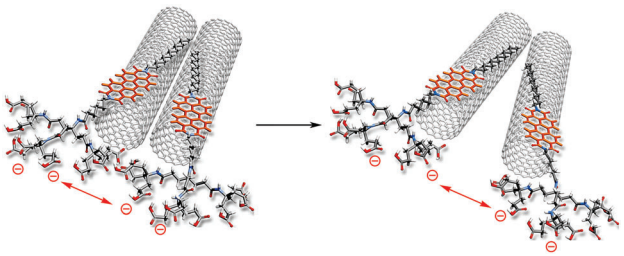

Figure 23. Schematic illustration of the separation of individual carbon nanotubes by PBI dispersion.

Dispersions of SWCNTs could also be obtained in organic solvents by using OEG dendrons (such as in PBI **32**) instead of Newkome dendrons. However, the stability of the PBI/SWCNT hybrids decreases as the size of the dendron substituents increases, because the steric demand and the hydrophilicity of the PBIs are increased.[107]

Noncovalent modification of SWCNTs offers several advantages. On the one hand, the molecular structure of the nanotubes and many of their intrinsic properties are preserved. On the other hand, the dispersion of nanotubes provides a way for their purification. As-synthesized SWCNTs are neither homogeneous nor well defined, but are instead mixtures of metallic and semiconducting tubes with varied lengths and diameters. After dispersion with water-soluble PBIs they can be purified and separated by ultracentrifugation.[108]

The examples discussed here impressively demonstrate that the π–π interaction of PBIs in water results in supramolecular structures with great potential applications in various fields, from materials science up to medicine.

6. Summary

Perylene bisimides (PBIs) are well-known for their versatile applications as pigments,[60] fluorescence dyes,[20] and n-semiconducting materials for organic electronics.[109,110] Thus, in the past few years enormous research effort has been focused on the development of PBI derivatives with greater solubility in organic solvents to enable easy purification and better processibility, and to achieve proper control of their arrangement in the solid state and supramolecular aggregates.[19] While PBIs have been established as an outstanding class of functional materials in these fields, their application in aqueous media was hardly investigated initially. Thus, the purpose of this Review is to illustrate that water is indeed a highly suitable solvent for this class of dyes and offers many opportunities, particularly in regard to self-assembled molecular aggregates, whose formation in the case of PBIs is driven by particularly strong hydrophobic interactions. Since π–π stacking interactions in water are not restricted to PBIs, this Review may also stimulate other studies in the field of supramolecular dye chemistry in aqueous media.

The concepts and strategies for supramolecular synthesis discussed in this Review have shown that PBIs can be made compatible with water as a solvent rather easily by the introduction of hydrophilic substituents. PBIs can be functionalized with water-solubility-mediating substituents at the imide as well as at the bay position, thus offering versatile opportunities for structural variations that are at best only rudimentarily explored so far. Water-soluble PBIs that are accessible by this approach possess strongly hydrophobic π surfaces, which can interact with themselves or with other π systems. The former process results in highly attractive macroscopic molecular assemblies such as micelles, vesicles, or nanofibers with numerous potential applications for materials research to artificial photosynthesis.[12c,111] It is quite encouraging that well-defined PBI dye aggregates and bilayer membranes can already be obtained in water, since the natural light-harvesting systems impressively illustrate the function and the benefit of highly organized membrane-bound dye aggregates.

Amongst the interactions of PBIs with other π systems, the dispersion of carbon nanotubes and graphenes stands out, as does the interactions with DNA. While the application of PBI-based fluorescence probes has been the topic of a previously published review in *Angewandte Chemie*,[24] the present Review illustrates how PBI-based molecular aggregates can contribute to a better understanding of the structure and physiological function of biomolecules such as DNA. Moreover, the examples discussed in this Review impressively demonstrate that the π–π interaction of PBIs with extended π surfaces of CNTs and graphene in water results in supramolecular structures with great potential for materials science up to photocatalytic application.[112] The topics of this Review represent high-priority research subjects, from which further interesting studies can be expected in the field of water-soluble π-conjugated chromophores in general and of perylene bisimides in particular.

We thank our former co-workers, who laid the foundations for the research work presented here, and our current co-workers, who are sharing the adventures related to the exploration of self-organization processes in water. We extend our particular thanks to Dr. Chantu R. Saha-Möller for correcting the manuscript and for providing the English translation. Financial support of our work by the Deutsche Forschungsgemeinschaft (grant Wu 317/11) and Alexander von Humboldt Foundation (postdoctoral fellowship for Xin Zhang) is greatly appreciated.

Received: December 9, 2011
Published online: May 9, 2012

[1] a) P. Ball, *Chem. Rev.* **2008**, *108*, 74 – 108; b) T. H. Lilley, *Philos. Trans. R. Soc. London B* **2004**, *359*, 1321 – 1322.
[2] Y. Zubavicus, M. Grunze, *Science* **2004**, *304*, 974 – 976.
[3] a) J. Kyte, *Biophys. Chem.* **2003**, *100*, 193 – 203; b) C. Tanford in *The Hydrophobic Effect: Formation of Micelles and Biological Membranes*, Wiley, New York, **1980**.
[4] S. Garde, A. J. Patel, *Proc. Natl. Acad. Sci. USA* **2011**, *108*, 16491 – 16492.
[5] D. Chandler, *Nature* **2005**, *437*, 640 – 647.
[6] D. Matulis, V. A. Bloomfield, *Biophys. Chem.* **2001**, *93*, 53 – 65.
[7] W. Blokzijl, J. B. F. N. Engberts, *Angew. Chem.* **1993**, *105*, 1610 – 1650; *Angew. Chem. Int. Ed. Engl.* **1993**, *32*, 1545 – 1579.
[8] a) E. A. Meyer, R. K. Castellano, F. Diederich, *Angew. Chem.* **2003**, *115*, 1244 – 1287; *Angew. Chem. Int. Ed.* **2003**, *42*, 1210 – 1250; b) H. Ringsdorf, B. Schlarb, J. Venzmer, *Angew. Chem.* **1988**, *100*, 117 – 162; *Angew. Chem. Int. Ed. Engl.* **1988**, *27*, 113 – 158.
[9] J. N. Israelachvili in *Intermolecular & Surface Forces, 2nd ed.*, Academic Press, San Diego, **1991**, pp. 122 – 394.
[10] a) D. González-Rodríguez, A. P. H. J. Schenning, *Chem. Mater.* **2011**, *23*, 310 – 325; b) F. Würthner, T. E. Kaiser, C. R. Saha-Möller, *Angew. Chem.* **2011**, *123*, 3436 – 3473; *Angew. Chem. Int. Ed.* **2011**, *50*, 3376 – 3410; c) D. M. Bassani, L. Jonusauskaite, A. Lavie-Cambot, N. D. McClenaghan, J. L. Pozzo, D. Ray, G. Vives, *Coord. Chem. Rev.* **2010**, *254*, 2429 – 2445.
[11] a) T. M. Figueira-Duarte, K. Müllen, *Chem. Rev.* **2011**, *111*, 7260 – 7314; b) W. Pisula, X. Feng, K. Müllen, *Chem. Mater.* **2011**, *23*, 554 – 567; c) J. E. Anthony, A. Facchetti, M. Heeney, S. R. Marder, X. Zhan, *Adv. Mater.* **2010**, *22*, 3876 – 3892; d) Z. Bao, J. Locklin in *Organic Field-Effect Transistors*, CRC, Boca Raton, **2007**; e) H. Klauk, in *Organic Electronics*, Wiley-VCH, Weinheim, **2006**; f) M. Schwoerer, H. C. Wolf in *Organische Molekulare Festkörper*, Wiley-VCH, Weinheim, **2005**.
[12] a) R. Bhosale, J. Míšek, N. Sakai, S. Matile, *Chem. Soc. Rev.* **2010**, *39*, 138 – 149; b) T. Hasobe, *Phys. Chem. Chem. Phys.* **2010**, *12*, 44 – 57; c) M. Wasielewski, *Acc. Chem. Res.* **2009**, *42*, 1910 – 1921; d) N. Aratani, D. Kim, A. Osuka, *Acc. Chem. Res.* **2009**, *42*, 1922 – 1934.
[13] C. A. Hunter, J. K. M. Sanders, *J. Am. Chem. Soc.* **1990**, *112*, 5525 – 5534.
[14] a) J.-H. Ryu, D.-J. Hong, M. Lee, *Chem. Commun.* **2008**, 1043 – 1054; b) Y.-b. Lim, M. Lee, *Org. Biomol. Chem.* **2007**, *5*, 401 – 405; c) B.-S. Kim, W.-Y. Yang, J.-H. Ryu, Y.-S. Yoo, M. Lee, *Chem. Commun.* **2005**, 2035 – 2037; d) B.-S. Kim, D.-J. Hong, J. Bae, M. Lee, *J. Am. Chem. Soc.* **2005**, *127*, 16333 – 16337.
[15] a) F. J. M. Hoeben, I. O. Shklyarevskiy, M. J. Pouderoijen, H. Engelkamp, A. P. H. J. Schenning, P. C. M. Christianen, J. C. Maan, E. W. Meijer, *Angew. Chem.* **2006**, *118*, 1254 – 1258; *Angew. Chem. Int. Ed.* **2006**, *45*, 1232 – 1236; b) M. Wolffs, F. J. M. Hoeben, E. H. A. Beckers, A. P. H. J. Schenning, E. W. Meijer, *J. Am. Chem. Soc.* **2005**, *127*, 13484 – 13485.
[16] a) F. García, L. Sánchez, *Chem. Eur. J.* **2010**, *16*, 3138 – 3146; b) F. García, G. Fernández, L. Sánchez, *Chem. Eur. J.* **2009**, *15*, 6740 – 6747.
[17] a) R. E. Hughes, S. P. Hart, D. A. Smith, B. Movaghar, R. J. Bushby, N. Boden, *J. Phys. Chem. B* **2002**, *106*, 6638 – 6645; b) T. Bast, R. Hentschke, *J. Phys. Chem.* **1996**, *100*, 12162 – 12171; c) N. Boden, R. J. Bushby, M. V. Jesudason, B. Sheldrick, *J. Chem. Soc. Chem. Commun.* **1988**, 1342 – 1343.
[18] a) G. Zhang, W. Jin, T. Fukushima, A. Kosaka, N. Ishii, T. Aida, *J. Am. Chem. Soc.* **2007**, *129*, 719 – 722; b) J. Wu, J. Li, U. Kolb, K. Müllen, *Chem. Commun.* **2006**, 48 – 50; c) W. Jin, T. Fukushima, A. Kosaka, M. Niki, N. Ishii, T. Aida, *J. Am. Chem. Soc.* **2005**, *127*, 8284 – 8285; d) J. P. Hill, W. Jin, A. Kosaka, T. Fukushima, H. Ichihara, T. Shimomura, K. Ito, T. Hashizume, N. Ishii, T. Aida, *Science* **2004**, *304*, 1481 – 1483.
[19] F. Würthner, *Chem. Commun.* **2004**, 1564 – 1579.
[20] a) C. Huang, S. Barlow, S. R. Marder, *J. Org. Chem.* **2011**, *76*, 2386 – 2407; b) H. Langhals, *Heterocycles* **2005**, *88*, 1309 – 1343; c) H. Langhals, *Heterocycles* **1995**, *40*, 477 – 500.
[21] a) W. E. Ford, *J. Photochem.* **1986**, *34*, 43 – 54; b) W. E. Ford, *J. Photochem.* **1987**, *37*, 189 – 204; c) H. Langhals, Deutsche Patentanmeldung, DE 3703513, **1987**; d) G. Schnurpfeil, J. Stark, D. Wöhrle, *Dyes Pigm.* **1995**, *27*, 339 – 350.
[22] a) T. Tang, A. Herrmann, K. Peneva, K. Müllen, S. E. Webber, *Langmuir* **2007**, *23*, 4623 – 4628; b) C. Kohl, T. Weil, J. Qu, K. Müllen, *Chem. Eur. J.* **2004**, *10*, 5297 – 5310; c) J. Qu, C. Kohl, M. Pottek, K. Müllen, *Angew. Chem.* **2004**, *116*, 1554 – 1557; *Angew. Chem. Int. Ed.* **2004**, *43*, 1528 – 1531.
[23] S. K. Yang, X. Shi, S. Park, S. Doganay, T. Ha, S. C. Zimmerman, *J. Am. Chem. Soc.* **2011**, *133*, 9964 – 9967.
[24] T. Weil, T. Vosch, J. Hofkens, K. Peneva, K. Müllen, *Angew. Chem.* **2010**, *122*, 9252 – 9278; *Angew. Chem. Int. Ed.* **2010**, *49*, 9068 – 9093.
[25] V. Percec, M. Peterca, T. Tadjiev, X. Zeng, G. Ungar, P. Leowanawat, E. Aqad, M. R. Imam, B. M. Rosen, U. Akbey, R. Graf, S. Sekharan, D. Sebastiani, H. W. Spiess, P. A. Heiney, S. D. Hudson, *J. Am. Chem. Soc.* **2011**, *133*, 12197 – 12219.
[26] Z. Chen, A. Lohr, C. R. Saha-Möller, F. Würthner, *Chem. Soc. Rev.* **2009**, *38*, 564 – 584.
[27] Z. Chen, B. Fimmel, F. Würthner, *Org. Biomol. Chem.* **2011**, DOI: 10.1039/C2OB07131B.
[28] a) H.-M. Zhao, J. Pfister, V. Settels, M. Renz, M. Kaupp, V. C. Dehm, F. Würthner, R. F. Fink, B. Engels, *J. Am. Chem. Soc.* **2009**, *131*, 15660 – 15668; b) R. F. Fink, J. Seibt, V. Engel, M. Renz, M. Kaupp, S. Lochbrunner, H.-M. Zhao, J. Pfister, F. Würthner, B. Engels, *J. Am. Chem. Soc.* **2008**, *130*, 12858 – 12859.
[29] Z. Chen, V. Stepanenko, V. Dehm, P. Prins, L. D. A. Siebbeles, J. Seibt, P. Marquetand, V. Engel, F. Würthner, *Chem. Eur. J.* **2007**, *13*, 436 – 449.
[30] X. Zhang, Z. Chen, F. Würthner, *J. Am. Chem. Soc.* **2007**, *129*, 4886 – 4887.
[31] a) T. Z. Mordasini Denti, W. F. van Gunsteren, F. Diederich, *J. Am. Chem. Soc.* **1996**, *118*, 6044 – 6051; b) D. B. Smithrud, F. Diederich, *J. Am. Chem. Soc.* **1990**, *112*, 339 – 343; c) D. B. Smithrud, T. B. Wyman, F. Diederich, *J. Am. Chem. Soc.* **1991**, *113*, 5420 – 5426.
[32] A. J. Zych, B. L. Iverson, *J. Am. Chem. Soc.* **2000**, *122*, 8898 – 8909.
[33] J. Seibt, T. Winkler, K. Renziehausen, V. Dehm, F. Würthner, H.-D. Meyer, V. Engel, *J. Phys. Chem. A* **2009**, *113*, 13475 – 13482.
[34] The excitonic coupling between PBI dyes has also been investigated in model systems which contained PBI dyes tethered by covalent spacers: a) H. Langhals, R. Ismael, *Eur. J. Org. Chem.* **1998**, 1915 – 1917; b) J. M. Giaimo, A. V. Gusev, M. R. Wasielewski, *J. Am. Chem. Soc.* **2002**, *124*, 8530 – 8531;

c) B. Rybtchinski, L. E. Sinks, M. R. Wasielewski, *J. Phys. Chem. A* **2004**, *108*, 7497 – 7505; d) C. Hippius, I. H. M. v. Stokkum, E. Zangrando, R. M. Williams, M. Wykes, D. Beljonne, F. Würthner, *J. Phys. Chem. C* **2008**, *112*, 14626 – 14638.

[35] J. B. Birks, *Rep. Prog. Phys.* **1975**, *38*, 903 – 974.

[36] M. Kasha, R. Rawls, M. A. El-Bayoumi, *Pure Appl. Chem.* **1965**, *11*, 371 – 392.

[37] T. Heek, C. Easting, C. Rest, X. Zhang, F. Würthner, R. Haag, *Chem. Commun.* **2010**, *46*, 1884 – 1886.

[38] B. Gao, H. Li, H. Liu, L. Zhang, Q. Bai, X. Ba, *Chem. Commun.* **2011**, *47*, 3894 – 3896.

[39] S. Rehm, V. Stepanenko, X. Zhang, T. H. Rehm, F. Würthner, *Chem. Eur. J.* **2010**, *16*, 3372 – 3382.

[40] Y. Liu, K.-R. Wang, D.-S. Guo, B.-P. Jiang, *Adv. Funct. Mater.* **2009**, *19*, 2230 – 2235.

[41] K.-R. Wang, D.-S. Guo, B.-P. Jiang, Z.-H. Sun, Y. Liu, *J. Phys. Chem. B* **2010**, *114*, 101 – 106.

[42] H. Langhals, W. Jona, F. Einsiedl, S. Wohnlich, *Adv. Mater.* **1998**, *10*, 1022 – 1024.

[43] C. D. Schmidt, C. Böttcher, A. Hirsch, *Eur. J. Org. Chem.* **2007**, 5497 – 5505.

[44] C. D. Schmidt, C. Böttcher, A. Hirsch, *Eur. J. Org. Chem.* **2009**, 5337 – 5349.

[45] a) H. Yin, Z. Zhou, J. Huang, R. Zheng, Y. Zhang, *Angew. Chem.* **2003**, *115*, 2238 – 2241; *Angew. Chem. Int. Ed.* **2003**, *42*, 2188 – 2191; b) P. Lesieur, M. A. Kiselev, L. I. Barsukov, D. Lombardo, *J. Appl. Crystallogr.* **2000**, *33*, 623 – 627.

[46] J. Leng, S. U. Egelhaaf, M. E. Cates, *Biophys. J.* **2003**, *85*, 1624 – 1646.

[47] a) B.-P. Jiang, D.-S. Guo, Y. Liu, *J. Org. Chem.* **2010**, *75*, 7258 – 7264; b) L. Zhang, A. Eisenberg, *J. Am. Chem. Soc.* **1996**, *118*, 3168 – 3181.

[48] a) H.-J. Kim, T. Kim, M. Lee, *Acc. Chem. Res.* **2011**, *44*, 72 – 82; b) J.-H. Ryu, H.-J. Kim, Z. Huang, E. Lee, M. Lee, *Angew. Chem.* **2006**, *118*, 5430 – 5433; *Angew. Chem. Int. Ed.* **2006**, *45*, 5304 – 5307; c) J. Bae, J.-H. Choi, Y.-S. Yoo, N.-K. Oh, B.-S. Kim, M. Lee, *J. Am. Chem. Soc.* **2005**, *127*, 9668 – 9669.

[49] T. Shimizu, M. Masuda, H. Minamikawa, *Chem. Rev.* **2005**, *105*, 1401 – 1443.

[50] O. Uzun, A. Sanyal, H. Nakade, R. J. Thibault, V. M. Rotello, *J. Am. Chem. Soc.* **2004**, *126*, 14773 – 14777.

[51] X. Zhang, S. Rehm, M. M. Safont-Sempere, F. Würthner, *Nat. Chem.* **2009**, *1*, 623 – 630.

[52] Y. Huang, J. Hu, W. Kuang, Z. Wei, C. F. J. Faul, *Chem. Commun.* **2011**, *47*, 5554 – 5556.

[53] Y. Huang, B. Quan, Z. Wei, G. Liu, L. Sun, *J. Phys. Chem. C* **2009**, *113*, 3929 – 3933.

[54] C. R. Weitzel, T. A. Everett, D. A. Higgins, *Langmuir* **2009**, *25*, 1188 – 1195.

[55] a) S.-W. Tam-Chang, J. Helbley, I. K. Iverson, *Langmuir* **2008**, *24*, 2133 – 2139; b) S.-W. Tam-Chang, I. K. Iverson, J. Helbley, *Langmuir* **2004**, *20*, 342 – 247.

[56] a) J. Lydon, *J. Mater. Chem.* **2010**, *20*, 10071 – 10099; b) S.-W. Tam-Chang, L. Huang, *Chem. Commun.* **2008**, 1957 – 1967.

[57] B. Rybtchinski, *ACS Nano* **2011**, *5*, 6791 – 6818.

[58] J. Baram, E. Shirman, N. Ben-Shitrit, A. Ustinov, H. Weissman, I. Pinkas, S. G. Wolf, B. Rybtchinski, *J. Am. Chem. Soc.* **2008**, *130*, 14966 – 14967.

[59] a) M. A. Iron, R. Cohen, B. Rybtchinski, *J. Phys. Chem. A* **2011**, *115*, 2047 – 2056; b) E. Shirman, A. Ustinov, N. Ben-Shitrit, H. Weissman, M. A. Iron, R. Cohen, B. Rybtchinski, *J. Phys. Chem. B* **2008**, *112*, 8855 – 8858.

[60] K. H. W. Herbst in *Industrial Pigments*: *Production*, *Properties*, *Applications*, *3rd ed.*, Wiley-VCH, Weinheim, **2004**.

[61] E. Krieg, E. Shirman, H. Weissman, E. Shimoni, S. G. Wolf, I. Pinkas, B. Rybtchinski, *J. Am. Chem. Soc.* **2009**, *131*, 14365 – 14373.

[62] E. Krieg, H. Weissman, E. Shirman, E. Shimoni, B. Rybtchinski, *Nat. Nanotechnol.* **2011**, *6*, 141 – 146.

[63] G. Golubkov, H. Weissman, E. Shirman, S. G. Wolf, I. Pinkas, B. Rybtchinski, *Angew. Chem.* **2009**, *121*, 944 – 948; *Angew. Chem. Int. Ed.* **2009**, *48*, 926 – 930.

[64] Y. Tidhar, H. Weissman, S. G. Wolf, A. Gulino, B. Rybtchinski, *Chem. Eur. J.* **2011**, *17*, 6068 – 6075.

[65] H. Weissman, A. Ustinov, E. Shimoni, S. R. Cohen, B. Rybtchinski, *Polym. Adv. Technol.* **2011**, *22*, 133 – 138.

[66] A. Ustinov, H. Weissman, E. Shirman, I. Pinkas, X. Zuo, B. Rybtchinski, *J. Am. Chem. Soc.* **2011**, *133*, 16201 – 16211.

[67] a) V. Urquidi, D. Tarin, S. Goodison, *Ann. Rev. Med.* **2000**, *51*, 65 – 79; b) C. H. Buys, *N. Engl. J. Med.* **2000**, *342*, 1282 – 1283; c) V. A. Zakian, *Science* **1995**, *270*, 1601 – 1607.

[68] C. Giovannangeli, T. Montenay-Garestier, M. Rougée, M. Chassignol, N. T. Thuong, C. Hélène, *J. Am. Chem. Soc.* **1991**, *113*, 7775 – 7777.

[69] a) D. Monchaud, M.-P. Teulade-Fichou, *Org. Biomol. Chem.* **2008**, *6*, 627 – 636; b) A. Arola, R. Vilar, *Curr. Topics Med. Chem.* **2008**, *8*, 1405 – 1415; c) S. M. Kerwin, *Curr. Pharm. Des.* **2000**, *6*, 441 – 471.

[70] a) M. Franceschin, *Eur. J. Org. Chem.* **2009**, 2225 – 2238; b) B. Tuesuwan, J. T. Kern, P. W. Thomas, M. Rodriguez, J. Li, W. M. David, S. M. Kerwin, *Biochemistry* **2008**, *47*, 1896 – 1909.

[71] O. Y. Fedoroff, M. Salazar, H. Han, V. V. Chemeris, S. M. Kerwin, L. H. Hurley, *Biochemistry* **1998**, *37*, 12367 – 12374.

[72] H. Han, C. L. Cliff, L. H. Hurley, *Biochemistry* **1999**, *38*, 6981 – 6986.

[73] A. Rangan, O. Y. Fedoroff, L. H. Hurley, *J. Biol. Chem.* **2001**, *276*, 4640 – 4646.

[74] H. Han, R. J. Bennett, L. H. Hurley, *Biochemistry* **2000**, *39*, 9311 – 9316.

[75] a) W. Tuntiwechapikul, T. Taka, M. Béthencourt, L. Makonkawkeyoon, T. R. Lee, *Bioorg. Med. Chem. Lett.* **2006**, *16*, 4120 – 4126; b) J. T. Kern, P. W. Thomas, S. M. Kerwin, *Biochemistry* **2002**, *41*, 11379 – 11389; c) S. M. Kerwin, G. Chen, J. T. Kern, P. W. Thomas, *Bioorg. Med. Chem. Lett.* **2002**, *12*, 447 – 450.

[76] a) L. Rossetti, M. Franceschin, S. Schirripa, A. Bianco, G. Ortaggi, M. Savino, *Bioorg. Med. Chem. Lett.* **2005**, *15*, 413 – 420; b) J. T. Kern, S. M. Kerwin, *Bioorg. Med. Chem. Lett.* **2002**, *12*, 3395 – 3398; c) L. Rossetti, M. Franceschin, A. Bianco, G. Ortaggi, M. Savino, *Bioorg. Med. Chem. Lett.* **2002**, *12*, 2527 – 2533.

[77] R. Samudrala, X. Zhang, R. M. Wadkins, D. L. Mattern, *Bioorg. Med. Chem.* **2007**, *15*, 186 – 193.

[78] L. Xue, N. Ranjan, D. P. Arya, *Biochemistry* **2011**, *50*, 2838 – 3849.

[79] a) M. Franceschin, E. Pasucci, A. Alvino, D. D'Ambrosio, A. Bianco, G. Ortaggi, M. Savino, *Bioorg. Med. Chem. Lett.* **2007**, *17*, 2515 – 2522; b) C. L. Mazzitelli, J. S. Brodbelt, J. T. Kern, M. Rodriguez, S. M. Kerwin, *J. Am. Soc. Mass Spectrom.* **2006**, *17*, 593 – 604.

[80] a) M. Franceschin, N. Borbone, G. Oliviero, V. Casagrande, M. Scuotto, T. Coppola, S. Borioni, L. Mayol, G. Ortaggi, A. Bianco, J. Amato, M. Varra, *Bioconjugate Chem.* **2011**, *22*, 1309 – 1319; b) S. Saha, J. Cai, D. Eiler, A. D. Hamilton, *Chem. Commun.* **2010**, *46*, 1685 – 1687.

[81] a) S. Bevers, S. Schutte, L. W. McLaughlin, *J. Am. Chem. Soc.* **2000**, *122*, 5905 – 5915; b) S. Bevers, T. P. Odea, L. W. McLaughlin, *J. Am. Chem. Soc.* **1998**, *120*, 11004 – 11005.

[82] Y. Zheng, H. Long, G. C. Schatz, F. D. Lewis, *Chem. Commun.* **2005**, 4795 – 4797.

[83] M. A. Abdalla, J. Bayer, J. O. Rädler, K. Müllen, *Angew. Chem.* **2004**, *116*, 4057 – 4060; *Angew. Chem. Int. Ed.* **2004**, *43*, 3967 – 3970.
[84] W. Wang, W. Wan, H.-H. Zhou, S. Niu, A. D. Q. Li, *J. Am. Chem. Soc.* **2003**, *125*, 5248 – 5249.
[85] C. Wagner, H.-A. Wagenknecht, *Org. Lett.* **2006**, *8*, 4191 – 4194.
[86] T. A. Zeidan, R. Carmieli, R. F. Kelley, T. M. Wilson, F. D. Lewis, M. R. Wasielewski, *J. Am. Chem. Soc.* **2008**, *130*, 13945 – 13955.
[87] H. Kashida, K. Sekiguchi, H. Asanuma, *Chem. Eur. J.* **2010**, *16*, 11554 – 11557.
[88] F. Menacher, H.-A. Wagenknecht, *Eur. J. Org. Chem.* **2011**, 4564 – 4570.
[89] D. Baumstark, H.-A. Wagenknecht, *Angew. Chem.* **2008**, *120*, 2652 – 2654; *Angew. Chem. Int. Ed.* **2008**, *47*, 2612 – 2614.
[90] F. Menacher, V. Stepanenko, F. Würthner, H.-A. Wagenknecht, *Chem. Eur. J.* **2011**, *17*, 6683 – 6688.
[91] a) M. Hariharan, Y. Zheng, H. Long, T. A. Zeidan, G. C. Schatz, J. Vura-Weis, M. R. Wasielewski, X. Zuo, D. M. Tiede, F. D. Lewis, *J. Am. Chem. Soc.* **2009**, *131*, 5920 – 5929; b) F. D. Lewis, L. Zhang, R. F. Kelley, D. McCamant, M. R. Wasielewski, *Tetrahedron* **2007**, *63*, 3457 – 3464.
[92] P. P. Neelakandan, Z. Pan, M. Hariharan, Y. Zheng, H. Weissman, B. Rybtchinski, F. D. Lewis, *J. Am. Chem. Soc.* **2010**, *132*, 15808 – 15813.
[93] M. Hariharan, K. Siegmund, Y. Zheng, H. Long, G. C. Schatz, F. D. Lewis, *J. Phys. Chem. C* **2010**, *114*, 20466 – 20471.
[94] R. Carmieli, T. A. Zeidan, R. F. Kelley, Q. Mi, F. D. Lewis, M. R. Wasielewski, *J. Phys. Chem. A* **2009**, *113*, 4691 – 4700.
[95] Y. Zheng, H. Long, G. C. Schatz, F. D. Lewis, *Chem. Commun.* **2006**, 3830 – 3832.
[96] F. Menacher, H.-A. Wagenknecht, *Photochem. Photobiol. Sci.* **2011**, *10*, 1275 – 1278.
[97] a) R. Varghese, H.-A. Wagenknecht, *Chem. Commun.* **2009**, 2615 – 2624; b) D. Baumstark, H.-A. Wagenknecht, *Chem. Eur. J.* **2008**, *14*, 6640 – 6645.
[98] T. A. Zeidan, M. Hariharan, K. Siegmund, F. D. Lewis, *Photochem. Photobiol. Sci.* **2010**, *9*, 916 – 922.
[99] a) S. M. Biner, D. Kummer, V. L. Malinovskii, R. Häner, *Org. Biomol. Chem.* **2011**, *9*, 2628 – 2633; b) R. Häner, S. M. Biner, S. M. Langenegger, T. Meng, V. L. Malinovskii, *Angew. Chem.* **2010**, *122*, 1249 – 1252; *Angew. Chem. Int. Ed.* **2010**, *49*, 1227 – 1230.
[100] N. Bouquin, V. L. Malinovskii, R. Häner, *Chem. Commun.* **2008**, 1974 – 1976.
[101] V. L. Malinovskii, D. Wenger, R. Häner, *Chem. Soc. Rev.* **2010**, *39*, 410 – 422.
[102] C. Backes, C. D. Schmidt, F. Hauke, C. Böttcher, A. Hirsch, *J. Am. Chem. Soc.* **2009**, *131*, 2172 – 2184.
[103] C. Ehli, C. Oelsner, D. M. Guldi, A. Mateo-Alonso, M. Prato, C. Schmidt, C. Backes, F. Hauke, A. Hirsch, *Nat. Chem.* **2009**, *1*, 243 – 249.
[104] C. Oelsner, C. Schmidt, F. Hauke, M. Prato, A. Hirsch, D. M. Guldi, *J. Am. Chem. Soc.* **2011**, *133*, 4580 – 4586.
[105] a) C. Backes, F. Hauke, A. Hirsch, *Adv. Mater.* **2011**, *23*, 2588 – 2601; b) C. Backes, C. D. Schmidt, K. Rosenlehner, F. Hauke, J. N. Coleman, A. Hirsch, *Adv. Mater.* **2010**, *22*, 788 – 802.
[106] J. M. Englert, J. Röhrl, C. D. Schmidt, R. Graupner, M. Hundhausen, F. Hauke, A. Hirsch, *Adv. Mater.* **2009**, *21*, 4265 – 4269.
[107] U. Hahn, S. Engmann, C. Oelsner, C. Ehli, D. M. Guldi, T. Torres, *J. Am. Chem. Soc.* **2010**, *132*, 6392 – 6401.
[108] a) C. D. Schmidt, A. Hirsch in *Advances in Synthetic Chemistry* (Ed.: B. Pignataro), Wiley-VCH, Weinheim, **2010**, pp. 283 – 304; b) C. Backes, F. Hauke, C. D. Schmidt, A. Hirsch, *Chem. Commun.* **2009**, 2643 – 2645.
[109] X. Zhan, A. Facchetti, S. Barlow, T. J. Marks, M. A. Ratner, M. R. Wasielewski, W. R. Marder, *Adv. Mater.* **2011**, *23*, 268 – 284.
[110] F. Würthner, M. Stolte, *Chem. Commun.* **2011**, *47*, 5109 – 5115.
[111] D. A. Doval, J. Areephong, E.-K. Bang, L. Bertone, P. Charbonnaz, A. Fin, N.-T. Lin, M. Lista, S. Matile, J. Montenegro, E. Orentas, N. Sakai, D.-H. Tran, A. V. Jentzsch, *Langmuir* **2011**, *27*, 9696 – 9705.
[112] D. M. Guldi, V. Sgobba, *Chem. Commun.* **2011**, *47*, 606 – 610.